^{186}Os and ^{187}Os enrichments and high-^{3}He/^{4}He sources in the Earth's mantle: Evidence from Icelandic picrites

Alan D. Brandon [a,*], David W. Graham [b], Tod Waight [c], Bjarni Gautason [d]

[a] Mail Code KR, NASA Johnson Space Center, Houston, TX 77058, USA
[b] College of Oceanic and Atmospheric Sciences, Oregon State University, Corvallis, OR 97331, USA
[c] Geological Institute, Øster Voldgade 10, 1350 Copenhagen K, Denmark
[d] Iceland Geosurvey and University of Akureyri, Rangarvellir, P.O. Box 30, 602 Akureyri, Iceland

Abstract

Picrites from the neovolcanic zones in Iceland display a range in ^{187}Os/^{188}Os from 0.1297 to 0.1381 (γ_{Os} = + 2.1 to +8.7) and uniform ^{186}Os/^{188}Os of 0.1198375 ± 32 (2σ). The value for ^{186}Os/^{188}Os is within uncertainty of the present-day value for the primitive upper mantle of 0.1198398 ± 16. These Os isotope systematics are best explained by ancient recycled crust or melt enrichment in the mantle source region. If so, then the coupled enrichments displayed in ^{186}Os/^{188}Os and ^{187}Os/^{188}Os from lavas of other plume systems must result from an independent process, the most viable candidate at present remains core–mantle interaction. While some plumes with high ^{3}He/^{4}He, such as Hawaii, appear to have been subjected to detectable addition of Os (and possibly He) from the outer core, others such as Iceland do not.

A positive correlation between ^{187}Os/^{188}Os and ^{3}He/^{4}He from 9.6 to 19 Ra in Iceland picrites is best modeled as mixtures of 1 Ga or older ancient recycled crust mixed with primitive mantle or incompletely degassed depleted mantle isolated since 1–1.5 Ga, which preserves the high ^{3}He/^{4}He of the depleted mantle at the time. These mixtures create a hybrid source region that subsequently mixes with the present-day convecting MORB mantle during ascent and melting. This multistage mixing scenario requires convective isolation in the deep mantle for hundreds of million years or more to maintain these compositionally distinct hybrid sources. The ^{3}He/^{4}He of lavas derived from the Iceland plume changed over time, from a maximum of 50 Ra at 60 Ma, to approximately 25–27 Ra at present. The changes are coupled with distinct compositional gaps between the different aged lavas when ^{3}He/^{4}He is plotted versus various geochemical parameters such as ^{143}Nd/^{144}Nd and La/Sm. These relationships can be interpreted as an increase in the proportion of ancient recycled crust in the upwelling plume over this time period.

The positive correlation between ^{187}Os/^{188}Os and ^{3}He/^{4}He demonstrates that the Iceland lava He isotopic compositions do not result from simple melt depletion histories and consequent removal of U and Th in their mantle sources. Instead their He isotopic compositions reflect mixtures of heterogeneous materials formed at different times with different U and Th concentrations. This hybridization is likely prevalent in all ocean island lavas derived from deep mantle sources.
Published by Elsevier Ltd.

1. INTRODUCTION

The ^{187}Re–^{187}Os and ^{190}Pt–^{186}Os isotopic systems have been valuable for tracing depths of origins of plumes and for constraining sources for mantle-derived magmas (Walker et al., 1995, 1997; Brandon et al., 1998, 1999, 2003; Puchtel et al., 2004, 2005; Brandon and Walker, 2005). The isotope ^{187}Re decays via beta emission to ^{187}Os with $\lambda = 1.67E^{-11}$ yr^{-1}, and ^{190}Pt decays via alpha emission to ^{186}Os with $\lambda = 1.48E^{-12}$ yr^{-1} (Smoliar et al., 1996; Begemann et al., 2001). Because ^{190}Pt is a minor isotope of Pt in combination with the small decay constant, this system is

---

* Corresponding author. Fax: +1 281 483 1573.
  E-mail address: alan.d.brandonl@jsc.nasa.gov (A.D. Brandon).

very insensitive to perturbations by most geochemical processes. Long-term and relatively large fractionations of Pt from Os are required to produce measurable differences in $^{186}Os/^{188}Os$ ratios. The outer core may have developed higher Pt/Os and Re/Os relative to chondrites and the Earth's mantle, owing to the crystallization of the inner core and leading to elevated $^{186}Os/^{188}Os$ and $^{187}Os/^{188}Os$ over time (Morgan et al., 1995; Walker et al., 1995). This is based on the assumption that these elements partition between solid metal and liquid metal in the Earth's core in a similar manner to their partitioning behavior in asteroidal cores where $D_{Os} > D_{Re} > D_{Pt}$ (D = solid metal/liquid metal bulk distribution coefficient). Recent experimental evidence on solid metal/liquid metal partitioning of Re, Os, and Pt supports the notion that the outer core evolves with elevated Re/Os and Pt/Os (Lauer and Jones, 1998; Walker, 2000; Chabot and Jones, 2003). Coupled enrichments in $^{186}Os/^{188}Os$ and $^{187}Os/^{188}Os$ have been found for some mantle-derived materials from three plume systems, the 251 Ma Siberian Traps, 89 Ma Gorgona Island, and present-day Hawaiian lavas, consistent with a small addition ($\sim$0.5 wt%) of outer core material into localized portions of the sources for these plumes (Brandon et al., 1998, 1999, 2003; Brandon and Walker, 2005).

The Hawaiian system in particular has provided important constraints on the origins of coupled $^{186}Os/^{188}Os$ and $^{187}Os/^{188}Os$ enrichments in some plume-derived magmas potentially resulting from core–mantle interaction and related to deep mantle sources. Elevated Fe/Mn ratios for the same samples measured for $^{186}Os/^{188}Os$ and $^{187}Os/^{188}Os$ is consistent with the addition of Fe metal into the source of the Hawaiian plume (Humayun et al., 2004). Alternatively, the incorporation of 10–20% mafic materials such as pyroxenite, or 1–3% Fe–Mn-rich sediment in the Hawaiian plume system could explain these Fe and Os isotope data (Smith, 2003; Baker and Jensen, 2004; Schersten et al., 2004). Thallium isotopes for these same samples indicate that admixture of $\sim$20 ppm Fe–Mn sediments with the ambient Hawaiian mantle may have occurred (Nielsen et al., 2006). These proportions of Fe–Mn sediments are several orders of magnitude too low to explain the elevated $^{186}Os/^{188}Os$ in some of the Hawaiian samples, and preclude them as a source for the coupled Os isotope enrichments (Brandon et al., 2003; Brandon and Walker, 2005; Nielsen et al., 2006). However, the issue of ancient mafic material, or other sediments that may be present in ancient recycled slabs, contributing to the coupled Os isotope enrichments remains unresolved. Brandon et al. (1998, 1999, 2003) showed that such materials had Pt/Re ratios that were ⩽15, too low to evolve over time to be the high $^{186}Os/^{188}Os$ and $^{187}Os/^{188}Os$ end-member needed to explain the linear mixing arrays for the Gorgonan, Siberian, and Hawaiian data. The Pt/Re ratios of the radiogenic Os isotope end-member must be ⩾80 to be consistent with the known geochemical behavior of Pt and Re during fractionation of solid metal leaving an evolved liquid, that could be in the outer core. Nevertheless, samples from additional plume systems need to be measured where geochemical evidence for ancient mafic and crustal materials in their mantle sources has been well established, in order to provide a test for the effects such material may have on the Os isotope budgets of plume systems.

Combined studies of Os and He isotopes have the potential to further unravel the source contributions to oceanic basalts and the origins of high $^{3}He/^{4}He$ in their mantle sources. A positive correlation between $^{186}Os/^{188}Os$ and $^{3}He/^{4}He$ previously observed in Hawaiian picritic lavas is consistent with a deep mantle origin of the coupled $^{187}Os–^{186}Os$ isotope signatures, and provides a potential link between Os and noble gas compositions in plume systems (Brandon et al., 1999). One possible source for primordial noble gas may be the outer core (Porcelli and Halliday, 2001). If this is the case, then samples from other high $^{3}He/^{4}He$ plume systems should also show correlated enrichments in $^{186}Os/^{188}Os$ and $^{187}Os/^{188}Os$. Another possibility is that the high $^{3}He/^{4}He$ signature results from partial outgassing of a lower mantle source that was originally primordial with respect to noble gases, but which was convectively isolated from the upper mantle during later stages of Earth history (Ballentine et al., 2005; Class and Goldstein, 2005). Such a high $^{3}He/^{4}He$ source may or may not produce a correlation with Os isotopes in plume-derived magmas, because the extent of correlation would depend on mixing between different domains within the plume source and during partial melting in the upper mantle. In another case, if high $^{3}He/^{4}He$ results from retention of He relative to U and Th during partial melting early in Earth history (Meibom and Anderson, 2004; Meibom et al., 2005; Parman, 2007), a negative correlation between $^{3}He/^{4}He$ and $^{187}Os/^{188}Os$ could be expected in the ambient upper mantle because of a corresponding lowering of Re/Os in the peridotite residue. This does not appear to be manifested in the sources for the Hawaiian picrites, but may be present in other magmatic systems. Finally, no correlation would be expected between He and Os isotopes if the source of coupled enrichments in $^{186}Os/^{188}Os$ and $^{187}Os/^{188}Os$ is from ancient mafic or crustal materials.

To provide additional tests for these issues, Os and He isotopic relationships are examined here for a suite of picrites that represent the range of geochemical variability from the neovolcanic zones in Iceland. These data are then compared with those from older magmatic rocks of the Iceland plume system in order to assess possible changes over time. The Iceland plume system is ideal for this examination because of the well-established high $^{3}He/^{4}He$ and the near-solar Ne isotopic compositions in many Iceland lavas. These noble gas characteristics likely require a deep mantle source that is distinct from the convecting upper mantle source for MORB (Kurz et al., 1982, 1985; Graham et al., 1998; Marty et al., 1998; Harrison et al., 1999; Hilton et al., 1999; Breddam et al., 2000; Dixon et al., 2000; Moreira and Sarda, 2000; Moreira et al., 2001; Stuart et al., 2003; Ellam and Stuart, 2004; Ballentine et al., 2005; Graham, 2005; Macpherson et al., 2005). In addition, there is evidence in some Icelandic lavas, from both noble gases and lithophile elements, for varying contributions from the upper mantle source for MORB as well as from several ancient crustal and/or mafic components within the mantle (Hemond et al., 1993; Hanan and Schilling, 1997; Fitton et al., 1997; Taylor et al., 1997; Stecher et al., 1999; Breddam et al., 2000; Chauvel and Hemond, 2000; Hanan et al., 2000; Kempton et al., 2000; Thirlwall et al., 2004;

Macpherson et al., 2005; Kokfelt et al., 2006; Thirlwall et al., 2006). These relationships are consistent with melting and mixing that accompanies the physical setting of the present-day Iceland plume beneath the spreading Mid-Atlantic Ridge system. This locality thereby provides a unique opportunity for systematic study of Os and He source contributions from both plume and convecting MORB mantle sources.

2. ANALYTICAL TECHNIQUES

Bulk-rock powders were analyzed by X-ray fluorescence for major and minor elements at the Geochemical Laboratories at McGill University on a Phillips PW2440 4 kW automated XRF spectrometer system with a Rhodium 60 kV end window X-ray tube (Table 1, Appendix A). The analyses were done on fused beads prepared from ignited samples. Analytical procedures are listed elsewhere (http://www.eps.mcgill.ca/~geochem/XRF_analytical_procedure2005.html). Bulk-rock powders were analyzed for trace elements at the University of Tasmania using a inductively coupled plasma mass spectrometer. Calibration was done with the USGS BHVO-1 standard, with other USGS rock standards run as quality control. Relevant data for this study are reported as trace element ratios in Table 1, and the remainder will be reported elsewhere.

The Nd isotopic analyses (Table 1) were carried out on a bulk rare earth element cut collected from conventional cation exchange columns. Analyses were run on the Axiom MC-ICPMS at the Danish Lithosphere Center (DLC) using methods similar to those described by Luais et al. (1997). The $^{143}Nd/^{144}Nd$ for the LaJolla standard was 0.511843 ± 10 ($n = 2$) and for the DLC/AMES standard was 0.512132 ± 11 (2σ, $n = 23$) during the analytical campaign where the Iceland picrites were analyzed.

Details of Re–Os analytical procedures have been previously documented (Brandon et al., 1999, 2000, 2003; Brandon et al., 2005a,b) and only a brief description is provided here. Rhenium and osmium concentration data (Table 2) were obtained on 2 g aliquots via isotope dilution. The sample powders were combined with a multi-Re–PGE (platinum group element) spike and loaded into Carius tubes with aqua regia and heated for 48 h at 250 °C. This insured sample-spike equilibrium for Os. Osmium was extracted from the aqua regia with CCl_4, and then back extracted into HBr. Osmium was then purified by microdistillation using chromic acid as an oxidant and HBr as a trap. The aqua regia was divided in half. One half was processed for PGE isotope dilution measurements. These data have been reported elsewhere (Humayun et al., 2002). The other half was processed for Re using anion exchange chemistry. Procedural blanks ran with the samples were 3.3 ± 0.5 pg for Os, with $^{187}Os/^{188}Os = 0.175 \pm 0.005$, and 46 ± 10 pg for Re. Blank corrections applied to Os concentrations were 0.12–2.0%, and to Re concentrations were 3–12%. The corrections for blank contribution on the $^{187}Os/^{188}Os$ ratio ranged from 0.00007 to 0.0009, depending on concentration of Os in each sample.

The spiked aliquots for Re and Os were measured on the Thermo Finnigan Triton thermal ionization mass spectrometer in negative ion mode (NTIMS) with the exception

of data for sample DMF 9101. The latter data were obtained at the University of Maryland Isotope Geochemistry Laboratory in 1999 using NTIMS and following procedures described elsewhere (Brandon et al., 1999). The Os cuts were loaded on to ultra-pure Pt filaments, with $Ba(OH)_2$. The spiked Os aliquots were measured on the SEM as OsO_3^- ions, in dynamic, peak-hopping mode. Ultra-pure, dry, oxygen pressure in the source was maintained at $1–3 \times 10^{-7}$ mbar for all measurements. Oxygen corrections were made using the oxygen isotopic composition measured on 2-ng loads of ReO_4^- on the Faraday cups. Instrumental mass fractionation corrections were applied using $^{192}Os/^{188}Os = 3.083$ and the exponential law. Four replicates of the Johnson Matthey Os standard during the analytical campaign gave $^{187}Os/^{188}Os = 0.11393 \pm 0.00026$ (2σ), within the range of accepted values (e.g., 0.1138067 ± 21, Brandon et al., 1999) and those for the high-precision, static Faraday cup runs described below. The Re cuts were loaded onto high purity Ni filaments with $Ba(NO)_3$ and measured in static mode on the faraday cups. Rhenium instrumental mass fractionation was estimated to be negligible based on the data for the in-house Re standard ($^{187}Re/^{185}Re = 1.6733 \pm 19$, 2σ). The concentration data for Re and Os, and $^{187}Os/^{188}Os$ for the spiked runs are reported in Table 1.

The unspiked aliquots were processed following the procedures described in Brandon et al. (1999, 2000, 2003) and briefly reported here. The goal was to obtain from 100 to 200 ng of Os to analyze for each measured sample. This required 100–1000 g of sample powder, depending on the Os concentration. The Ni–S fire assay technique was employed to purify Os. The NiS blebs containing concentrated Os are dissolved in 12 N HCl, and insoluble Os sulfide is trapped on cellulose paper by filtering the HCl solution. The Os-bearing cellulose is dissolved in a Carius tube using reverse aqua regia, and Os is purified using the procedures listed above for the spiked samples.

High-precision Os isotope data for unspiked aliquots of DMF9101 was obtained via NTIMS at the University of Maryland following the measurement protocol outlined previously (Brandon et al., 1998, 1999, 2000, 2003). The remainder of the high-precision Os isotope data were obtained by NTIMS on the Thermo Finnigan Triton (Table 2). The data were obtained in static mode using seven Faraday collectors. Signal intensities of 120–180 mV on mass 234 ($^{186}Os^{16}O_3^-$) and 235 ($^{187}Os^{16}O_3^-$) were generated for $\geqslant 180$ ratios to reach run precision of ± 0.0000026 or better ($2\sigma_{mean}$) for the $^{186}Os/^{188}Os$ ratio. Each cycle had an integration time of 17 s followed by a 4 s settling time. The isobaric interference of $^{186}W^{16}O_3^-$ on $^{186}Os^{16}O_3^-$ was monitored by measuring $^{184}Os^{16}O_3^-$ ($^{184}W^{16}O_3^-$). This interference has not been observed on this Triton during Os measurements which is consistent with the very different ionization behaviors of W and Os negative oxide species. (Brandon et al., 2003; Puchtel et al., 2004, 2005; Brandon et al., 2005a,b; Walker et al., 2005). Oxygen corrections were made using the oxygen isotopic composition obtained for 2 ng loads of ReO_4 on the Faraday cups as listed above. Only one bottle of oxygen was used during the analytical campaign that included all samples listed in Table 1. Repeated

Table 1
Iceland sample locales and compositional parameters considered in this paper

Sample	Location	Latitude	Longitude	Rock Type	MgO (wt%)	FeO_T	Mg#	$(La/Sm)_n$	$(Th/Sm)_n$	$(Th/La)_n$	ΔNb[d]	$^{143}Nd/^{144}Nd$
ICE 0	NRZ[a]—Hruthalsar	65°19.500′	16°30.000′	Picrite	20.11	9.02	0.799	0.50	0.34	0.69	0.195	0.513121(07)
ICE 2	WRZ[b]—Lagafell	63°53.104′	22°32.200′	Picrite	20.72	8.41	0.815	0.35	0.13	0.37	0.193	0.513147(06)
ICE 3	WRZ—Stapafell	63°54.633′	22°31.343′	Picrite	18.00	11.11	0.743	1.60	0.87	0.54	0.321	0.512999(06)
ICE 4a	WRZ—Maelifell	64°06.685′	21°11.755′	Picrite	25.27	9.89	0.820	0.45	0.17	0.38	0.096	0.513103(07)
ICE 4b	WRZ—Maelifell	64°06.685′	21°11.755′	Picrite	23.85	9.81	0.813	0.46	0.17	0.38	0.102	0.513100(06)
ICE 5	WRZ—Dagmalafell	64°10.484′	21°02.910′	Picrite	18.76	9.64	0.776	0.43	0.15	0.34	0.236	0.513064(07)
DMF 9101	WRZ—Dagmalafell	64°10.533′	21°02.800′	Picrite	22.37	9.73	0.804	0.45	0.15	0.33	0.212	0.513062(07)
ICE 6	NRZ—Theistareykir	65°57.580′	17°04.129′	Picrite	12.48	9.53	0.700	0.56	0.22	0.40	0.069	0.513102(06)
ICE 8a	ERZ[c]—Skridufell	64°07.009′	19°56.811′	Picrite	15.62	11.22	0.713	1.78	1.64	0.92	0.049	0.513039(06)
ICE 8b	ERZ—Skridufell	64°07.009′	19°56.811′	Picrite	19.27	10.99	0.758	1.82	1.82	1.00	0.040	0.513036(06)
ICE 9a	ESZ—Skridufell	64°07.009′	19°56.811′	Picrite	12.96	11.37	0.670	1.69	1.50	0.88	0.045	0.513031(07)
ICE 10	WRZ—Hrudurkarlarnir	64°31.267′	20°52.561′	Picrite	12.33	9.52	0.698	0.83	0.55	0.67	0.370	0.513053(07)
ICE 11	WRZ—Grindarik	63°50.171′	22°24.960′	Picrite	17.38	8.23	0.790	0.31	0.11	0.35	0.193	0.513087(06)
9805	WRZ—Haleyjabunga	63°49.183′	22°39.150′	Picrite	28.47	8.37	0.858	0.33	0.06	0.20	0.007	0.513119(13)
9806	WRZ—Vatnsheidi	63°50.650′	22°23.483′	Picrite	15.17	8.28	0.766	0.72	0.33	0.46	0.350	0.513038(06)
9809	WRZ—Fagradalshraun	63°54.700′	22°17.683′	Picrite	24.78	8.96	0.831	0.37	0.11	0.29	0.027	0.513126(07)
9810	WRZ—Eldborg	63°51.350′	22°00.117′	Basalt	10.70	11.49	0.624	1.26	0.63	0.50	0.307	0.513038(06)
9812	WRZ—Asar	63°54.533′	21°23.867′	Picrite	15.95	8.18	0.777	0.36	0.13	0.36	0.165	0.513114(07)
9815	WRZ—Lyngfell	63°51.517′	22°18.717′	Basalt	9.47	10.76	0.611	1.50	0.79	0.52	0.355	0.513009(07)

Error bars for Nd isotope ratios listed in parentheses are $\pm 2\sigma$ for the last decimal place. The trace elements are normalized to CI chondrites (Anders and Grevesse, 1989).

[a] NRZ—Northern Rift Zone.
[b] WRZ—Western Rift Zone.
[c] ERZ—Eastern Rift Zone.
[d] $\Delta Nb = 1/75 + \log(Nb/Y) - 1.92\log(Zr/Y)$ (Fitton et al., 1997).

Table 2
Iceland Re–Os isotopic data

Sample	Re	Os	$^{187}Os/^{188}Os^a$	$^{187}Re/^{188}Os$	$^{184}Os/^{188}Os^b$	$^{186}Os/^{188}Os^b$	$^{187}Os/^{188}Os^b$
ICE 0 Hruthalsar	612.3	863.2	0.12941(15)	3.42	0.0013109(15)	0.1198382(18)	0.1297040(20)
ICE 2 Lagafell	305.7	1053.0	0.13109(24)	1.40	0.0013088(12)	0.1198386(14)	0.1323100(14)
ICE 3 Stapafell	355.5	123.6	0.13168(26)	13.86			
ICE 4a Maelifell	493.9	457.1	0.13335(20)	5.21	0.0013266(24)	0.1198376(24)	0.1326225(26)
ICE 4b Maelifell	615.5	881.6	0.13315(14)	3.37	0.0013101(17)	0.1198369(17)	0.1327022(17)
ICE 5 Dagmalafell	459.8	410.9	0.13305(20)	5.40			
DMF 9101 Dagmalafell[c]	352.6	746.3	0.13208(19)	2.28	0.001313(1)	0.1198350(48)	0.1324049(12)
ICE 6 Theistareykir	711.8	139.9	0.13467(21)	24.54	0.0013139(19)	0.1198359(21)	0.1352774(27)
ICE 8a Skridufell	487.3	273.5	0.13716(24)	8.59	0.0013076(13)	0.1198404(16)	0.1371644(16)
ICE 8b Skridufell	279.7	516.4	0.13750(22)	2.61	0.0013089(23)	0.1198369(23)	0.1376726(23)
ICE 9a Skridufell	476.1	148.2	0.13784(22)	15.49	0.0013084(14)	0.1198367(18)	0.1381292(18)
ICE 10 Hrudurkarlarnir	432.4	183.8	0.13140(20)	11.34			
ICE 11 Grindarik	390.7	877.1	0.13116(24)	2.15	0.0013109(23)	0.1198390(24)	0.1318350(19)
9805 Haleyjabunga	152.3	1064.9	0.13151(21)	0.689	0.0013122(19)	0.1198365(19)	0.1319716(22)
9806 Vatnsheidi	357.8	674.2	0.13278(22)	2.56			
9809 Fagradalshraun	336.6	1028.3	0.13081(31)	1.58	0.0013157(16)	0.1198410(17)	0.1308974(17)
9810 Eldborg	585.9	62.9	0.13518(31)	44.92			
9812 Asar	496.0	424.2	0.13406(19)	5.64	0.0013108(19)	0.1198381(21)	0.1340553(26)
9815 Lyngfell	573.5	203.7	0.13586(21)	13.58	0.0013065(24)	0.1198371(26)	0.1344091(31)
Johnson–Matthey std.							
1					0.0013194(25)	0.1198520(29)	0.1137986(33)
2					0.0013125(17)	0.1198513(19)	0.1138026(19)
3					0.0013088(19)	0.1198522(22)	0.1137990(22)
4					0.0013113(23)	0.1198518(22)	0.1138000(20)
5					0.0013102(24)	0.1198503(27)	0.1137952(29)
6					0.0013192(20)	0.1198535(24)	0.1138042(22)

Concentrations of Re and Os are in parts per trillion. Reported uncertainties in parentheses are $\pm 2\sigma$ for the last decimal place.

[a] Isotopic compositions obtained from spiked aliquots.
[b] Isotopic compositions obtained from unspiked aliquots.
[c] Measurements for DMF 9101 performed at University of Maryland.

measurements for the oxygen isotopic composition using Re indicated no change over time. The oxygen pressure for all runs was maintained in the range of $2–3 \times 10^{-7}$ mbar. After oxygen corrections were made on the raw data, instrumental mass fractionation corrections were performed using the exponential law and $^{192}Os/^{188}Os = 3.083$. The mean of six runs of the Johnson–Matthey Os standard during the analytical campaign was 0.0013136 ± 38 for $^{184}Os/^{188}Os$, 0.1198518 ± 23 for $^{186}Os/^{188}Os$ and 0.1137999 ± 64 for $^{187}Os/^{188}Os$ ($\pm 2\sigma$). The average for $^{186}Os/^{188}Os$ on the Johnson–Matthey standard during this analytical campaign was higher than previously measured at the University of Maryland and on this Triton of $^{186}Os/^{188}Os = 0.1198475$ (Walker et al., 1997; Brandon et al., 1998; Brandon et al., 1999; Brandon et al., 2000; Brandon et al., 2003; Puchtel et al., 2004; Brandon et al., 2005a,b; Puchtel et al., 2005; Walker et al., 2005). Accordingly, for direct comparison to earlier data, the Iceland picrite and basalt data in Table 1 were corrected to the $^{186}Os/^{188}Os$ ratio of 0.1198475 of the Johnson–Matthey standard obtained in the earlier studies.

For He analyses, details of the procedures are presented elsewhere (Graham et al., 1998). Olivine and glass separates were analyzed for He trapped in melt/fluid inclusions by in vacuo crushing using approximately 200 high impact strokes. The reported 2σ errors (Table 4) include in-run analytical uncertainties, plus those associated with air standards and blank corrections.

3. RESULTS

The Iceland samples studied here are primarily picrites and picritic basalts with olivine phenocrysts. The samples come from widely dispersed locales within the neovolcanic zones (Table 1 and Fig. 1), ranging from Theistareykir and Hruthalsar in the Northern Rift Zone (NRZ), to Skridufell in the Eastern Rift Zone (ERZ), and 13 locales in the Western Rift Zone (WRZ). The MgO contents range from 9.5% to 28.5% wt% (Table 1). The Mg#'s (calculated with all Fe as FeO) range from 0.61 to 0.86. The samples have from 4 to 32 vol % olivine phenocrysts. The samples range from light rare earth element (LREE) depleted with $(La/Sm)_n$ of 0.31 to enriched with $(La/Sm)_n$ of 1.82 (normalized to CI chondrites, Anders and Grevesse, 1989). The $(Th/Sm)_n$ ratios also range from depleted with 0.11 to enriched with 1.82 (Table 1). All of the samples have ΔNb values of >0, consistent with their occurrence from Iceland and distinct from samples erupted in surrounding regions that have ΔNb values of <0 (Fitten et al., 1997). The Nd isotopic compositions range from 0.512999 to 0.513147 (ε_{Nd} from 7.0 to 9.9), typical for neovolcanic zone Iceland lavas (Taylor et al., 1997; Kempton et al., 2000; Thirlwall et al., 2004).

Samples ICE 5 and DMF 9101 were obtained during separate field campaigns from the same quarry at Dagmalafell, Midfell. Samples ICE 4a and 4b are from adjacent outcrops
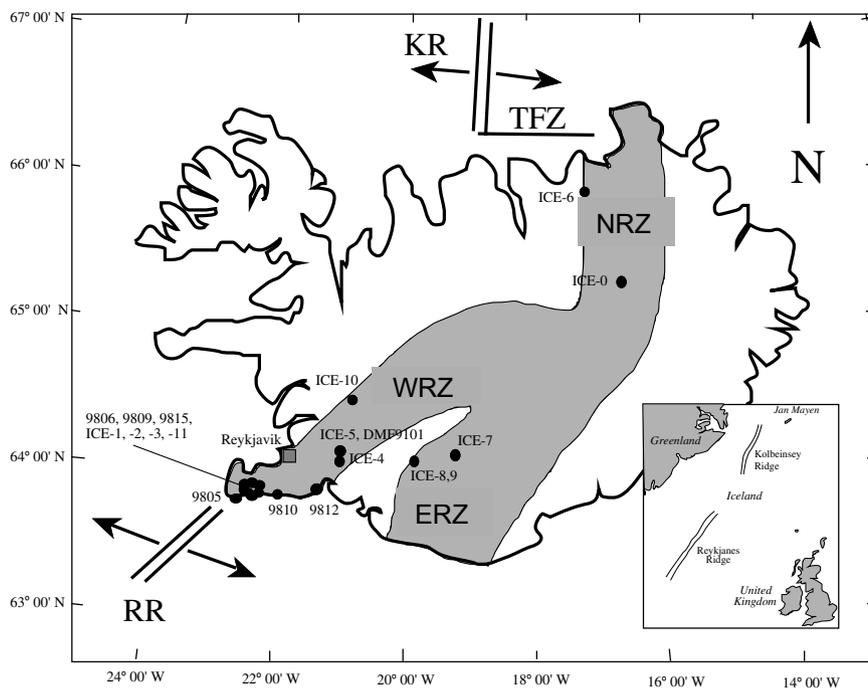
Fig. 1. Map of Iceland and showing the sample locations for this study as well as zones of active volcanism as shaded regions. Abbreviations are as follows: RR, Reykjanes Ridge; KR, Kolbeinsey Ridge; TFZ, Tjornes Fracture Zone; WRZ, Western Rift Zone; ERZ, Eastern Rift Zone; NRZ, Northern Rift Zone.

at Maelifell, while ICE 8a and 8b are from the same flow at Skrudufell. The different samples from each locale display differing major element compositions relative to each other as a result of variable amounts of olivine phenocrysts and potentially other fractionating phases, that were the result of differentiation subsequent to extraction from the mantle (e.g., MgO and Mg#, Table 1; Brandon et al., 2001). The reproducibilities of lithophile trace element ratios and isotopic data for these duplicate samples from the same locales show that these compositional parameters are independent of shallow level processes that may affect these magmas, such as crustal assimilation and concomitant or subsequent crystal fractionation (Tables 1–3).

Concentrations of Re and Os for the Iceland picrites and basalts analyzed in this study are comparable to those for other picrite suites such as those from Hawaii. For example, Bennett et al. (1996) and Brandon et al. (1999) reported a range of Re concentrations from 181 to 1093 ppt, and Os concentrations from 465 to 1083 ppt, for a suite of Hawaiian picrites. The Iceland samples studied here have Re from 152 to 712 ppt and Os from 63 to 1065 ppt (Table 2), similar to the range of Os concentrations previously reported for nine Iceland picrites (Skovgaard et al., 2001). Osmium concentrations correlate inversely with $^{187}Re/^{188}Os$ but scatter with $^{187}Os/^{188}Os$ (Fig. 2). The $^{187}Re/^{188}Os$ ratios range from 0.7 to 44.9, and show a rough correlation with decreasing MgO (Fig. 3; and Mg#, not shown). The $^{187}Os/^{188}Os$ ratios range from 0.1297 to 0.1381 and scatter with MgO (Fig. 3). These relationships are consistent with the compatible and incompatible behavior of Os and Re, respectively, during fractionation and olivine accumulation. The lack of correlation of $^{187}Os/^{188}Os$ with any differentia-

tion indices implies that the Os isotopic composition of these magmas was set prior to any residence in the Icelandic crust and thus cannot be a function of crustal assimilation. This is consistent with additional evidence presented in the preceeding paragraph and below, that the geochemical features of these lavas reflect their mantle source regions.

High precision Os isotopic measurements for picrites and basalts from the neovolcanic zones in Iceland, ranging from southern locales in the Rekjyanes Peninsula in the WRZ to one sample in the NRZ in the Theistareykir area are listed in Table 2. A $^{186}Os/^{188}Os$ of 0.1198350 ± 48 (2σ) was obtained for sample DMF 9101 at University of Maryland. A range of $^{186}Os/^{188}Os$ from 0.1198359 ± 21 to 0.1198410 ± 17 was measured for 13 samples on the Triton. This range of values is slightly greater than the external precision based on replicate measurements of the standard, which for this study, was ±0.0000023 (2σ).

Helium concentrations and $^{3}He/^{4}He$ ratios for olivine and glass from the samples measured in this study are reported in Table 3. He isotope data are reported relative to the atmospheric $^{3}He/^{4}He$ ratio of 1.39×10^{-6} (Ra), using the R/Ra notation. In addition, He data published elsewhere, for samples that come from the same outcrops or lava flows as those in the present study, are also listed. Samples ICE 5 and DMF 9101 come from a quarry at Dagmalafell, Midfell, and have $^{3}He/^{4}He$ values of 16.4 ± 0.51 and 17.20 ± 0.09 Ra for olivine and glass, respectively (Table 1). These data compare well with values of 16.5 and 17.5 Ra measured in glass samples from this quarry and reported elsewhere (Harrison et al., 1999).

For the samples measured in this study, $^{3}He/^{4}He$ ranges from 9.6 Ra for ICE 0 in the NRZ, to 17.2 Ra for ICE 8b in

Table 3
He isotope and concentration data for Iceland picrites

Sample	Wt (mg)	Phase	^{3}He/^{4}He (R/Ra)	±2σ	[He] (nccSTP/g)[d]
ICE 0 Hruthalsar	535.0	Olivine	9.62	0.63	1.14
ICE 2 Lagafell	452.1	Olivine	11.18	1.63	3.90
		Olivine	*14.09[a]*	*0.14*	*1.53*
ICE 3 Stapafell		*Glass*	*13.9[a]*		*1430*
ICE 4a Maelifell	650.6	Olivine	11.46	0.32	5.36
ICE 5 Dagmalafell	548.5	Olivine	16.62	0.26	12.2
	362.5	Glass	17.20	0.09	2560
DMF 9101 Dagmalafell	530.4	Olivine	16.40	0.51	11.7
		Glass	*16.50[b]*	*0.97*	*512*
		Glass	*17.53[b]*	*1.25*	*258*
ICE 8b Skridufell	619.0	Olivine	17.30	0.25	37.3
ICE 10 Hrudurkarlarnir	500.7	Olivine	12.76	0.74	1.16
9805 Haleyjabunga		*Olivine*	*10.89[a]*	*0.60*	*0.52*
9806 Vatnsheidi		*Olivine*	*11.65[a]*	*0.22*	*4.26*
9809 Fagradalshraun	629.5	Olivine	12.74	0.46	1.92
9810 Eldborg		*Olivine*	*19.0[c]*	*2*	*13.0*
9812 Asar	225.9	Olivine	16.80	2.15	0.61
9815 Lyngfell	496.1	Olivine	15.83	0.59	3.48

New results from this study, with the weight of olivine or glass analyzed, are for helium extractions by in vacuo crushing. Previous results from the literature are reported in italics.
[a] Breddam et al. (2000).
[b] Harrison et al. (1999), average of $n = 11$, and $n = 5$.
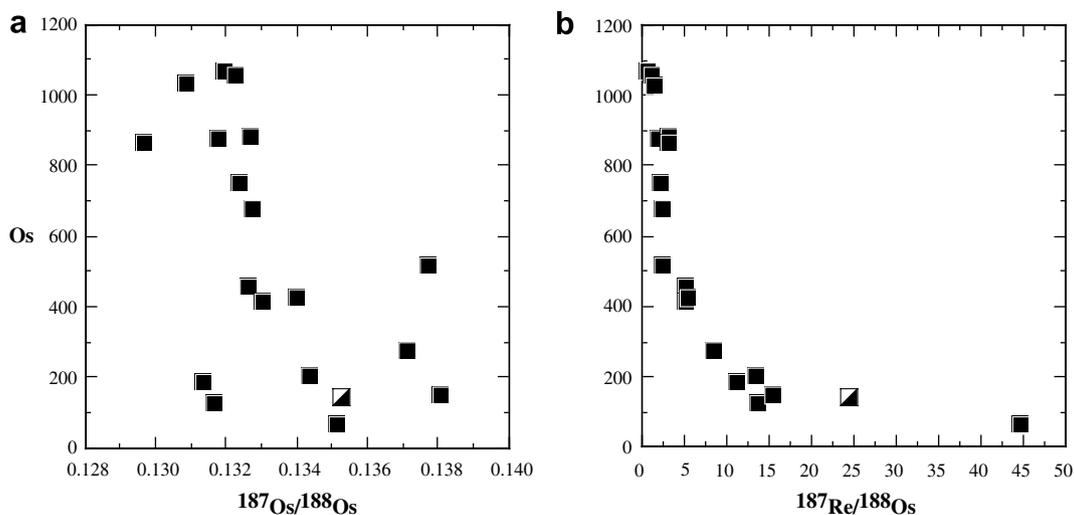[c] Dixon (2003).
[d] nccSTP/g = 10^{-9} ccSTP/g.

Fig. 2. (a) ^{187}Os/^{188}Os–Os for Iceland picrites. The half filled square is sample ICE 6 from Theistareykir, all other samples are solid squares. (b) ^{187}Re/^{188}Os–Os.

the ERZ. The Eldborg basalt flow studied here has a previously reported ^{3}He/^{4}He = 19 ± 2 Ra (Dixon, 2003). Published data for Iceland lavas within the neovolcanic zones have ^{3}He/^{4}He ranging from 8.0 to 21 Ra (Breddam et al., 2000; Macpherson et al., 2005; and references therein), with one glass sample having a value as high as 26 Ra (Kurz et al., 1985). A single sample containing both clinopyroxene and olivine shows values of 20.2 ± 10 and 34.3 ± 8 Ra (2σ, Macpherson et al., 2005), but given the low He concentrations and large analytical uncertainties, the significance of the high ^{3}He/^{4}He in this sample is unclear. Hence, the sam-

ples in this study have ^{3}He/^{4}He that span the range reported previously for samples from the neovolcanic zones in Iceland, with the exception of two samples having ^{3}He/^{4}He > 21 Ra, as noted.

4. DISCUSSION

4.1. Mantle sources for Os

The average ^{186}Os/^{188}Os for the 13 Iceland samples measured on the Triton is 0.1198375 ± 32 (2σ). This value is
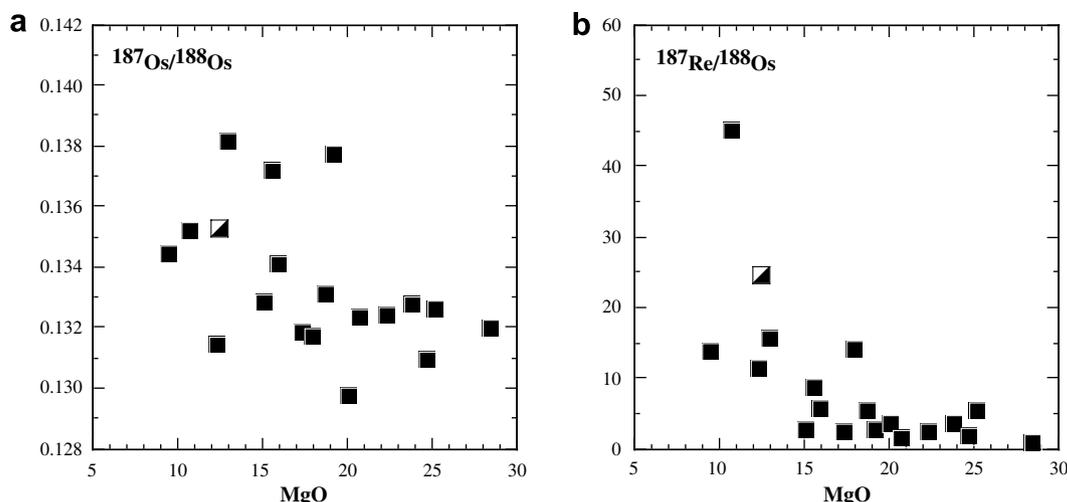
Fig. 3. (a) MgO–$^{187}Os/^{188}Os$ for Iceland picrites. Sample symbols as in Fig. 2. (b) MgO–$^{187}Re/^{188}Os$.

within uncertainty of the estimated present-day primitive mantle (PM) value for $^{186}Os/^{188}Os$ of 0.1198398 ± 16 (2σ), recently established by Brandon et al. (2006) on new measurements of chondrites, komatiites, and mantle-derived Os-rich alloys. The $^{187}Os/^{188}Os$ ratios for the Iceland samples in this study range from 0.1297 to 0.1381. This range extends from the present-day estimated value for PM of 0.1296 ± 0.0008 (Meisel et al., 2001) to more radiogenic values. This limited range of $^{186}Os/^{188}Os$ similar to PM combined with a wide range in $^{187}Os/^{188}Os$ for the Iceland picrites is in contrast the relationships between $^{186}Os/^{188}Os$ and $^{187}Os/^{188}Os$ for samples from other Phanerozoic plume systems, namely the 251 Ma Siberian, 89 Ma Gorgonan, and the recent Hawaiian systems. The samples from these three locales have coupled enrichments in $^{186}Os/^{188}Os$ and γOs (where $\gamma Os = [(^{187}Os/^{188}Os_{sample@t}/$ $^{187}Os/^{188}Os_{chondrite@t} - 1) * 100]$, present-day $^{187}Os/$ $^{188}Os_{chondrite} = 0.1270$, and $^{187}Re/^{188}Os_{chondrite} = 0.4083$, Shirey and Walker, 1998) relative to PM (Fig. 4). Hence, the coupled radiogenic $^{186}Os/^{188}Os$ and $^{187}Os/^{188}Os$ component that is manifested in the samples from the other three plume systems is absent in the Iceland samples.

The enrichment in $^{187}Os/^{188}Os$ with no variation in $^{186}Os/^{188}Os$ relative to a present day chondritic upper mantle has important implications for the origins of Os isotopic variation in mantle-derived materials. Unlike the samples from Siberia, Gorgona, and Hawaii that require a radiogenic end-member with long-term superchondritic Pt/Os, Re/Os, and Pt/Re, the Iceland picrites show that a radiogenic end-member with long-term superchondritic Re/Os is present in their source, but no long-term superchondritic Pt/Os or Pt/Re is manifested in the $^{186}Os/^{188}Os$ ratios. For example, ancient basaltic components that were formed at 2 and 1 Ga from a primitive upper mantle, evolve over time with shallow vectors in $^{186}Os/^{188}Os$ versus $^{187}Os/^{188}Os$, as a result of strong Re enrichment with only minor Pt enrichment (Fig. 4). Such a radiogenic component can explain not only the $^{187}Os/^{188}Os$ in the Iceland picrite data, but also that needed for other mantle-derived materials that display Re-enrichments in their sources. Other types of crustal

materials thought to be present in ancient subducted slabs plot with similar shallow vectors in this diagram (Brandon et al., 1999). This is consistent with observations on Os-rich alloys found in mantle samples in ophiolites associated with subduction zone settings (Brandon et al., 2006). Given the revised estimate for the PM for $^{186}Os/^{188}Os$ of 0.1198398 ± 16, a source having long-term Re-enrichment with no Pt-enrichment is also necessary to explain the Hawaiian end-member represented by Mauna Kea lavas (with $^{186}Os/^{188}Os = 0.119835$ and $\gamma Os = 2$) as well as for the Koolau end-member (with $^{186}Os/^{188}Os = 0.119835–0.119840$ and $\gamma Os \geqslant 8$) (Brandon et al., 1999; Fig. 4) that both plot to the right of the time evolution curve for PM. Trace element ratios, and lithophile isotopic compositions for the Kea compositional end-member indicate that its source underwent melt depletion in the past, followed by an enrichment overprint consistent with the constraints from Os isotopes in Fig. 4 where Re is an incompatible element (Hauri, 1996; Hofmann and Jochum, 1996; Eiler et al., 1998).

These Os isotope systematics for the Iceland picrites are consistent with additional geochemical evidence for ancient recycled slab components in the mantle sources for Iceland magmas (Hemond et al., 1993; Hanan and Schilling, 1997; Taylor et al., 1997; Stecher et al., 1999; Hanan et al., 2000; Chauvel and Hemond, 2000; Kempton et al., 2000; Thirlwall et al., 2004; Macpherson et al., 2005; Thirlwall et al., 2006). Ancient melt enrichment processes and/or additions of recycled crust to the mantle source generate radiogenic $^{187}Os/^{188}Os$ in lavas and mantle peridotites with no resolvable effects on $^{186}Os/^{188}Os$ (Fig. 4). The absence of $^{186}Os/^{188}Os$ enrichments in Iceland is, in turn, strong evidence that some other process produces the coupled enrichments of $^{186}Os/^{188}Os$ and $^{187}Os/^{188}Os$ observed at other mantle plume localities. The observation that these coupled Os isotope enrichments occur independently of both melt enrichment processes or the presence of ancient recycled crust in their mantle sources is further support for an origin from core–mantle interaction. These new data for the Iceland picrites suggest that core–mantle interaction is a
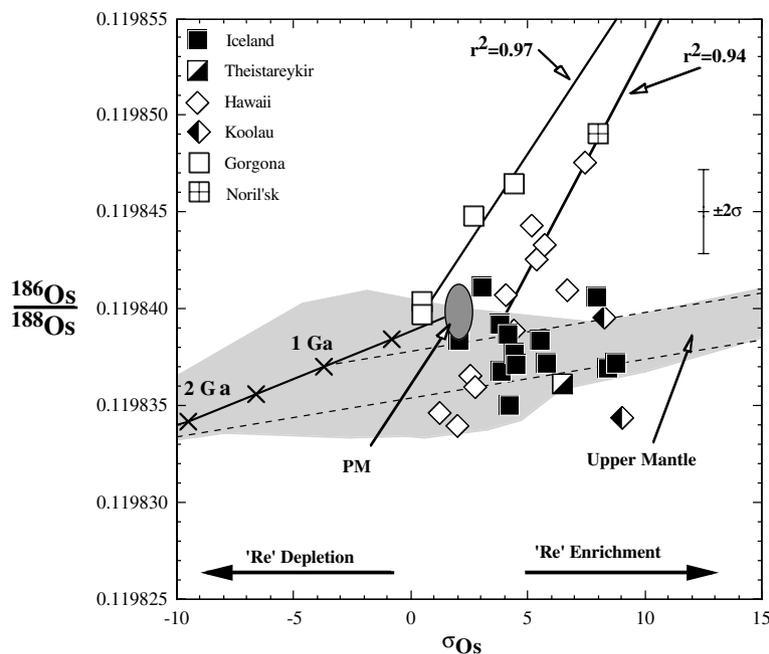
Fig. 4. γOs versus $^{186}Os/^{188}Os$ for Iceland picrites, Hawaiian picrites, 89 Ma Gorgona komatiites, and 251 Ma Siberian sample, where $\gamma Os = [(^{187}Os/^{188}Os_{sample@t}/^{187}Os/^{188}Os_{chondrite@t} - 1) * 100]$, present-day $^{187}Os/^{188}Os_{chondrite} = 0.1270$, and $^{187}Re/^{188}Os_{chondrite} = 0.4083$ (Shirey and Walker, 1998). The field for global upper mantle samples is shown as a shaded region, the primitive mantle (PM) evolution curve is shown with 500 Ma increments to the present-day value, dashed lines extending to the right from the PM curve are for mafic material evolution trends formed from a PM reservoir at 1 and 2 Ga (Brandon et al., 2006). Regression lines through the Gorgonan and Hawaiian–Siberian trends are shown with calculated r^2s (Brandon et al., 1999, 2003). Typical $\pm 2\sigma$ uncertainty for the data is shown in the upper right of the diagram.

localized process and unlikely to be prevalent in all plume source regions (Brandon et al., 2003; Brandon and Walker, 2005). While some plumes with high $^3He/^4He$, such as Hawaii, appear to have been subjected to detectable addition of Os from the outer core, others such as Iceland do not.

4.2. Origins of Os–He variation: the role of ancient recycled lithosphere and high $^3He/^4He$ sources

One of the most interesting geochemical features of this suite of Iceland picrites is the strong positive correlation of $^{187}Os/^{188}Os$ with $^3He/^4He$ (Fig. 5a). This correlation ranges from $^{187}Os/^{188}Os = 0.1297$ and $^3He/^4He = 9.6$ Ra, typical for upper mantle material, to $^{187}Os/^{188}Os \sim 0.1381$ and $^3He/^4He \sim 19$ Ra. This correlation defies standard explanation because as shown above, the radiogenic $^{187}Os/^{188}Os$ indicates a source with a high time-integrated Re/Os ratio, characteristic of ancient recycled crust or melt-enriched lithospheric mantle. The presence of such material in the mantle source should not lead to high $^3He/^4He$ a priori. Recent experiments for olivine/melt pairs suggest that He may sometimes behave as a slightly more compatible element than U or Th during partial melting (Parman et al., 2005), but the relative behaviors are only crudely understood and it seems just as likely, if not more so, that He behaves overall more incompatibly than U and Th during partial melting of peridotite or pyroxenite. The high $^{187}Os/^{188}Os$ lavas in Iceland also have superchondritic

La/Sm (Fig. 5b) and Th/Sm, with chondritic Th/La (Fig. 6) consistent with a lithophile trace element-enriched source. This should lead to ^4He accumulation in the source resulting from decay of ^{238}U, ^{235}U, and ^{232}Th, with consequent low $^3He/^4He$ that is in contrast to the high $^3He/^4He$ observed for the lavas that have the strongest signals for enrichment (Figs. 5 and 6). In addition to the correlation between $^{187}Os/^{188}Os$, $^3He/^4He$ and the trace element ratios observed here, the high $^3He/^4He$ source for neovolcanic zone Iceland lavas may also have a low $\delta^{18}O$ relative to MORB mantle (Thirlwall et al., 2006).

In the following sections, models are formulated, based on the Os–He isotope systematics, to account for these features. The goal is to reproduce the positive trend observed in Fig. 5a as mixing between MORB mantle with $^{187}Os/^{188}Os \leqslant 0.1296$ and $^3He/^4He \leqslant 8$ Ra with a single source component having high $^{187}Os/^{188}Os$ and $^3He/^4He$. Realistic parameters are input into a mixing model to create a hybrid mantle source that is constructed as an end-member composition having elevated $^3He/^4He \geqslant 25$ Ra (the maximum value established for Iceland neovolcanic zone lavas) and $^{187}Os/^{188}Os \geqslant 0.1381$ (the maximum value measured in this study, Table 2). The modeling approach taken, which we consider the most straightforward, is to mix ancient recycled crust with hypothetical mantle compositions having elevated $^3He/^4He$. One of the key parameters considered is to assess the possible age of ancient recycled material. In order to account for the Pb isotopic systematics of Iceland neovolcanic zone lavas that have a negative
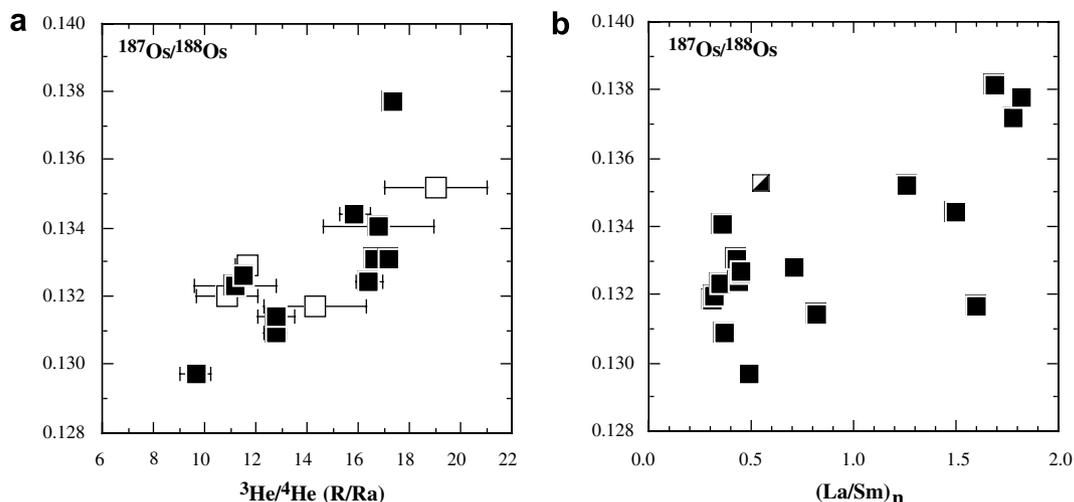
Fig. 5. (a) ^{3}He/^{4}He–^{187}Os/^{188}Os for Iceland picrites. Solid symbols are for samples where He was measured in the present study, open symbols for those taken from the literature from the same locales (Table 3). Error bars for ^{3}He/^{4}He are ±2σ. (b) (La/Sm)$_n$–^{187}Os/^{188}Os.

Δ^{207}Pb (deviation of ^{207}Pb/^{204}Pb for a given ^{206}Pb/^{204}Pb relative to the Northern Hemisphere Reference Line), Thirlwall et al. (2004) suggested that such material in the Iceland mantle would form with a higher U/Pb ratio relative to the MORB mantle at a time as young as 170 Ma ago. In contrast, Kokfelt et al. (2006) suggests that recycled lithosphere of ∼1.5 Ga can account for the Pb isotopic signatures of neovolcanic zone lavas. Hence, constraining the age of the recycled material or time of melt-enrichment to account for geochemical features of Iceland neovolcanic zone lavas is crucial for any viable model. The parameters chosen for the models are constrained in the following two sections, followed by evaluation of the models in the third section.

4.2.1. He constraints

Values of ^{3}He/^{4}He for the high Ra Icelandic mantle source range from the maximum ^{3}He/^{4}He measured in mantle-derived volcanic rocks from the Iceland plume at 60 Ma (^{3}He/^{4}He = 50 Ra, Stuart et al., 2003), to a lower value of 37 Ra, based on a measurement of a Tertiary lava from Iceland (Hilton et al., 1999). In order to minimize the amount of ancient recycled crust necessary to create a hybrid component having 25–33 Ra, values as low as 37 Ra are used for the high Ra end-member. This approach is taken because constraining the minimum amount of crust necessary at any given time of formation will evaluate ^{187}Os/^{188}Os–^{3}He/^{4}He relations in the context of having a relatively young recycled component of several hundred Ma and possibly as low as 170 Ma as noted above (Thirlwall et al., 2004).

The He systematics for a high Ra source are modeled for two end-member scenarios. In the first scenario, estimates of an incompletely degassed depleted mantle (IDDM) He source follows Class and Goldstein (2005), where this source has an initial ^{3}He = 3.54×10^{-13} mol/g and a corresponding ^{4}He of 1.11×10^{-9} mol/g at 230 Ra, following an initial stage of outgassing during Earth accretion to 4.4 Ga. This equates to [He] = 24.8 μcc(STP)/g. If this source

remained closed for He over earth history, it would evolve from 230 Ra at 4.4 Ga to 95 Ra at present as a result of U and Th decay producing ^{4}He. In the Class and Goldstein (2005) model, the mantle is progressively melted until 2.7 Ga to create continental crust and complementary IDDM, with consequent loss of U and Th and outgassing of He. Following 2.7 Ga, IDDM has MORB mantle values for U and Th/U of 4.7 and 2.91ppb, respectively, and continues to evolve to lower ^{3}He/^{4}He and outgas He. In this approach, the present-day ^{3}He/^{4}He for any mantle source is marked by its formation age, the time at which it becomes isolated from the shallow convecting mantle, and stops outgassing He, plus the addition of ^{4}He from U and Th decay. In the case where this source continues to outgas He, it evolves to the present-day composition of MORB mantle with ^{3}He/^{4}He = 8 Ra (Fig. 7). Three different model examples of IDDM are used here—having isolation ages of 1.5 Ga, 1.0 Ga, and 750 Ma, with initial ^{3}He/^{4}He of 103, 81.7, and 65.5 Ra, and evolving to 72.5, 50.9, and 37 Ra at present, respectively (Table 4). The present-day He concentrations for these three sources are 5.35, 2.70, and 1.71 μcc(STP)/g, respectively (Table 4).

In a second scenario, a primordial source evolves from 4.4 Ga with 230 to 37 Ra at present, with no fractionation between U, Th, and He (Fig. 7). For example, a source with 230 Ra at 4.4 Ga and bulk silicate Earth U and Th/U of 21 ppb and 4.05, respectively, would require an initial amount of ^{3}He of 9.58×10^{-14} mol/g and a corresponding ^{4}He content of 3.00×10^{-10} mol/g (6.72 μcc(STP/g) to evolve to 37 Ra at present and having 41.7 μcc(STP)/g (primitive mantle (PM), Table 4). This source has an initial inventory of He that is 60% less than the estimate of a primordial source of Class and Goldstein (2005), but because it is assumed that there is no outgassing or removal of U and Th by partial melting over Earth history, its evolution leads to a present day He content that is a factor of 24 higher compared to IDDM with 37 Ra (Table 4). There are clearly large uncertainties associated with both 37 Ra sources, and hence the He concentrations should be viewed
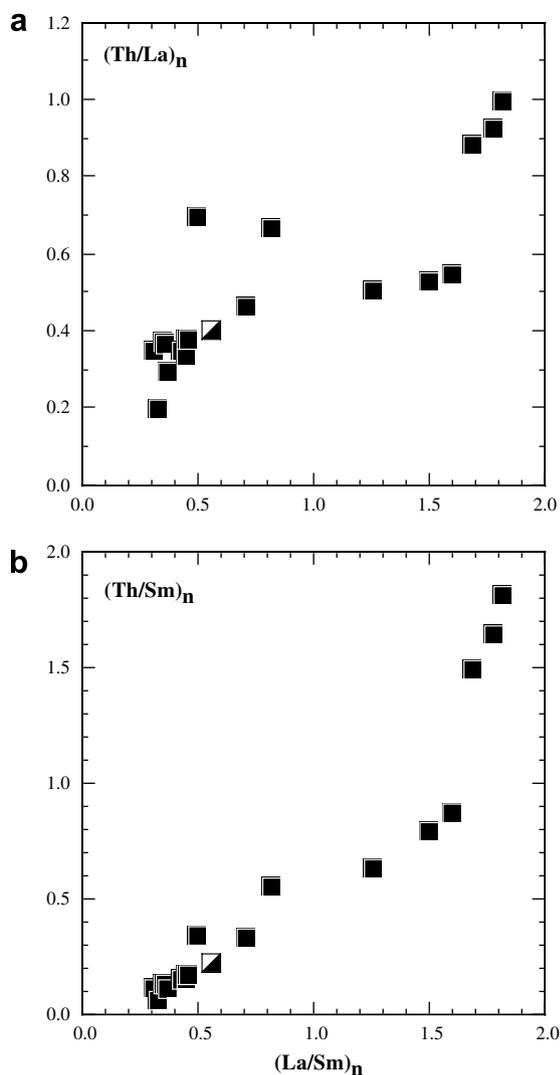
Fig. 6. (a) $(La/Sm)_n$–$(Th/La)_n$ for Iceland picrites. Sample symbols as in Fig. 2. (b) $(La/Sm)_n$–$(Th/Sm)_n$.

Fig. 7. The He isotopic composition (a) and [He] in μcc(STP)/g (b) for evolving high Ra plume sources from 4.4 Ga to present. The primitive mantle (PM) source is for an undegassed source that evolves from 230 to 37 Ra at present. The incompletely degassed depleted mantle (IDDM) source is the model of Class and Goldstein (2005). Model IDDM sources isolated at 750 Ma, 1 Ga, and 1.5 Ga are shown. The present-day compositions of IDDM isolated at any time is the $^3He/^4He$ and [He] values plotting along the initial IDDM source curve at the isolation age plus accumulation of ^4He from U and Th decay from that age to present-day. For example IDDM isolated at 1.5 Ga with 103 Ra will evolve to 72 Ra at present. Present-day parameters for the two end-member high $^3He/^4He$ sources, and 3 IDDM sources isolated at 750 Ma, 1 Ga, and 1.5 Ga are listed in Table 4. See text for further discussion.

as time-integrated approximations. These two end-member scenarios, having significantly different He concentrations resulting from strong outgassing and melt depletion in one case, and little or no outgassing and melt depletion in a second case, serve to constrain possible origins of the high $^3He/^4He$ signature in the Iceland lavas. Does the high $^3He/^4He$ reflect isolation in the past from the shallow depleted mantle, or does it reflect a source containing remnants more similar to primordial mantle having elevated ^3He contents? The outcomes of the models presented below bear directly on this question.

The He concentrations for ancient recycled crust components depend on a number of factors, including the amount of degassing at or near the time of formation, the concentrations of U and Th, and time for ^4He ingrowth. This is complicated further by the potential loss of He, U, and Th during dehydration and heating of subducted slabs under volcanic arcs (Dodson and Brandon, 1999; Becker et al., 2000; Plank et al., 2002; Kelley et al., 2005; Kessel et al., 2005). The basaltic portions of fresh oceanic crust
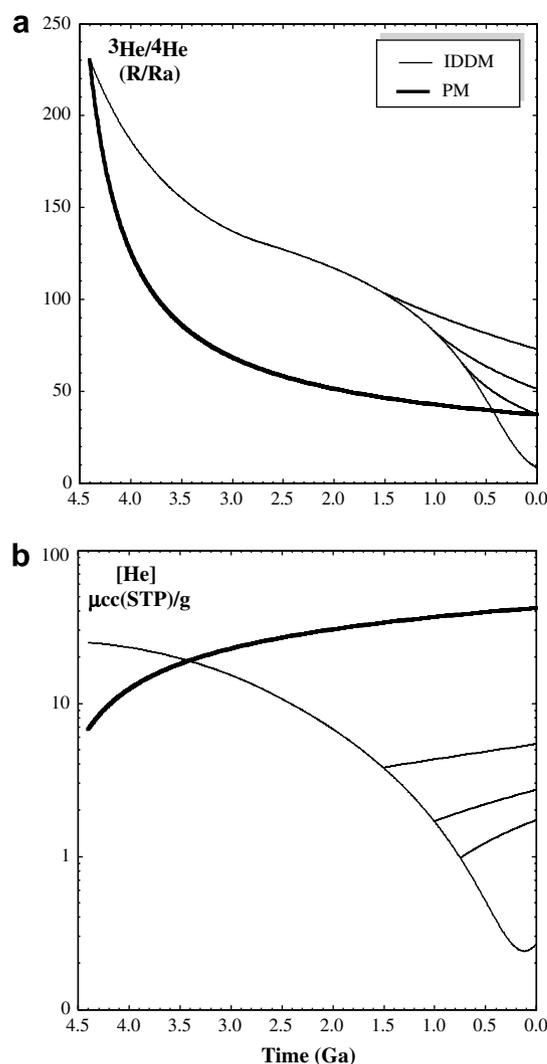
have U and Th concentrations ranging from 50 to 120 ppb, and 70 to 190 ppb, respectively, with a Th/U of approximately 3, while altered basaltic crust is estimated to have U and Th concentrations of 300 and 187 ppb, respectively (Hofmann, 1988; Wedepohl and Hartmann, 1994; Staudigel et al., 1996; Hart et al., 1999). The U and Th concentrations for dehydrated eclogites ($T > 900 °C$) have been estimated to be 117 and 168 ppb, representing

Table 4
End-member components used to model the He–Os isotope systematics

Component	Os (ppb)	Re (ppb)	Pt (ppb)	Re/Os	Pt/Re	$^{187}Os/^{188}Os$	U (ppb)	Th/U	He μcc(STP)/g	$^{3}He/^{4}He$ R/Ra
Primitive mantle (PM)	3.0	0.27	6.0	0.09	22.2	0.12960	21.0[c]	4.05[c]	41.7	37
MORB mantle depleted and degassed at 0 Ma[a]	3.3	0.20	4.5	0.06	22.5	0.12500	4.7[d]	2.91[d]	0.269	8.0
Incompletely degassed depleted mantle (IDDM) at 750 Ma[a]	3.3	0.20	4.5	0.06	22.5	0.12500	4.7	2.91	1.7	37
Incompletely degassed depleted mantle (IDDM) at 1 Ga[a]	3.3	0.20	4.5	0.06	22.5	0.12500	4.7	2.91	2.7	50.9
Incompletely degassed depleted mantle (IDDM) at 1.5 Ga[a]	3.3	0.20	4.5	0.06	22.5	0.12500	4.7	2.91	5.35	72.5
250 Ma basalt	0.0097[b]	0.423	0.596	43.7	1.41	1.122	100	3	5.22[e]	0.43[e]
500 Ma Ga basalt	0.0108[b]	0.423	0.596	39.2	1.41	2.118	100	3	10.6[e]	0.80[e]
1 Ga basalt	0.0130[b]	0.423	0.596	32.4	1.41	4.121	100	3	22.2[e]	2.30[e]
2 Ga basalt	0.0176[b]	0.423	0.596	24.1	1.41	8.172	100	3	49.6[e]	5.94[e]
250 Ma reduced sed.	0.3503[b]	40.26	1.16	115.0	0.029	3.446	840	4.1	50.0[e]	0.01
500 Ga reduced sed.	0.4564[b]	40.26	1.16	88.3	0.029	6.775	840	4.1	102[e]	0.01
1 Ga reduced sed.	0.6693[b]	40.26	1.16	60.2	0.029	13.449	840	4.1	210[e]	0.01
2 Ga reduced sed.	1.101[b]	40.26	1.16	35.6	0.029	27.001	840	4.1	454[e]	0.01
250 Ma slab = 5% sed. + 95% basalt	0.0267	2.415	0.624	80.8	0.259	2.515	137	3.34	7.46	3.12
1 Ga slab = 5% sed. + 95% basalt	0.0459	2.415	0.624	52.6	0.259	9.731	137	3.34	31.6	1.06
2 Ga slab = 5% sed. + 95% basalt	0.0717	2.415	0.624	33.7	0.259	19.470	137	3.34	69.8	0.526

See text for additional data sources and explanation.

[a] Class and Goldstein (2005).

[b] The initial Os concentrations at 0.25, 0.50, 1, and 2 Ga for basalt and reduced sediment are 0.00856 and 0.244 ppb, respectively. Present-day Os concentrations of these components reflect ingrowth of radiogenic ^{186}Os and ^{187}Os from formation time to present.

[c] Sun and McDonough (1989).

[d] Salters and Stracke (2004).

[e] The He concentrations and $^{3}He/^{4}He$ are for basalt that was initially outgassed by 99%, and for sediment that was completely outgassed, and lost 50% of its U and Th relative to a starting composition of GLOSS (U = 1.68 ppm, Th/U = 4.1) during subduction.

approximately 60% and 10% removal, respectively, of these two elements during subduction processes from altered basaltic portions of slabs (Becker et al., 2000). Hence, for calculating ^{4}He production over time in basaltic portions of slabs, a U concentration of 100 ppb and Th/U of 3 is used, that approximates the average of both unaltered and dehydrated lithologies.

For the basaltic portions of ocean crust, the initial ^{3}He/^{4}He will depend on the time of crust extraction from the upper mantle and the present-day ^{3}He/^{4}He will depend on the degree of outgassing and in-situ decay of U and Th. Fig. 8a shows the ^{3}He/^{4}He for basalt formed from IDDM from 2.0 Ga to present and degree of outgassing from 0%
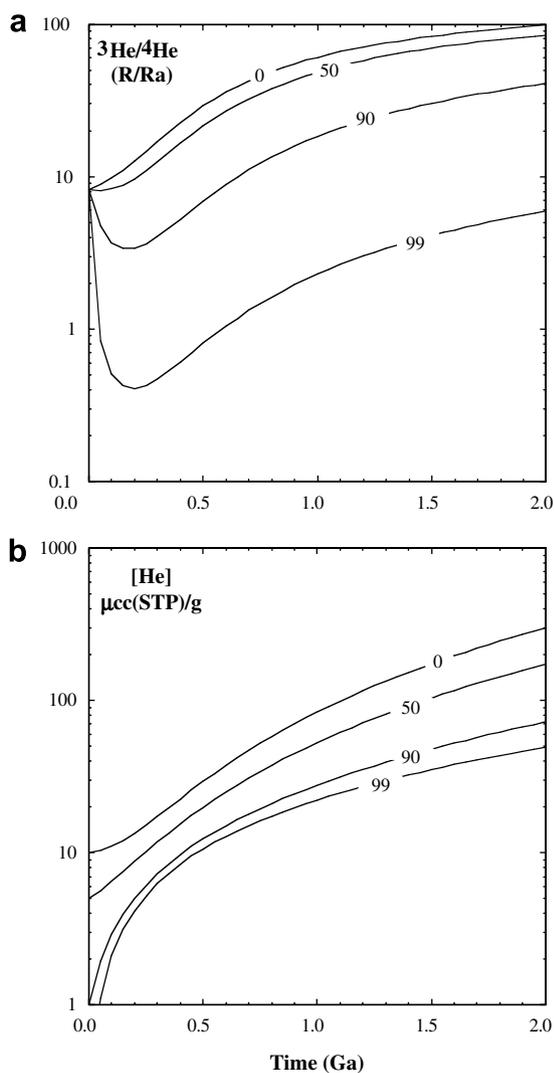

Fig. 8. The He isotopic composition (a) and [He] in μcc(STP)/g (b) of ancient recycled seafloor ranging in age from 0 to 2 Ga, calculated using initial ^{3}He/^{4}He, U abundances, and Th/U listed in Table 4. For the basalt, the curves represent undegassed (i.e., 0%), and 50%, 90%, and 99% of outgassing of endogenous He closely following the time of formation of ocean crust. It is highly unlikely that ocean crust remains 0% degassed when subducted, hence the outgassing curves are more realistic of ancient recycled materials. See text for additional discussion.

to 99%. The calculated present-day concentrations for the basalt crust formed at 2.0 Ga to present are shown in Fig. 8b. The initial concentration for a basalt at a specified time in the past is calculated assuming a constant concentration ratio of 37.2 between basalt and source. This is obtained from MORB glass with 10 μcc(STP)/g (Graham, 2002) and present-day IDDM (i.e., equivalent to DMM, or MORB mantle) source of 0.269 μcc(STP)/g from the Class and Goldstein (2005) model. Because IDDM is progressively higher in He concentration with older ages (Fig. 7), the basalt derived from this source will also be proportionally higher in initial He. As illustrated by the curves for different degrees of outgassing in Fig. 8, the amount of outgassing of the crust during its formation is crucial for calculating the composition and ^{3}He/^{4}He for a slab of any given age contributing to present-day magmatism. Ancient slabs that underwent little to as much as 90% outgassing can have present-day ^{3}He/^{4}He ratios that are higher than the modern MORB mantle, along with high concentrations of He (Fig. 8). However, in a characterization of lower ocean crust, Moreira et al. (2003) found that the He concentrations were ≤0.25 μcc(STP)/g, much less than those shown in Fig. 8b. Furthermore, even the basaltic upper crust will be very degassed given its highly crystalline nature compared to the thin glassy sections of basalts that are typically analyzed for MORB noble gas studies. Moreira et al. (2003) also found that the Ne isotopic compositions of these samples were similar to atmospheric Ne ratios. Without extensive noble gas removal during subduction, ancient slabs would control the Ne budget of the upper mantle imparting an atmospheric composition, which is not observed. Hence, the combination of He and Ne results show that ocean slabs are extensively outgassed. Thus for the mixing models presented below, the basalt is considered to be 99% outgassed for any age of formation, and ^{4}He is therefore primarily a function of ^{4}He build-up from U and Th decay. These are considered to be maximum He concentrations and ^{3}He/^{4}He given the constraints from the Moreira et al. (2003) study.

Ocean sediments have U and Th concentrations ranging from ~0.05 to 7 and ~0.07 to 18 ppm, respectively, with widely varying Th/U from 0.2 to 10 (Klinkhammer and Palmer, 1991; Plank and Langmuir, 1998; Plank et al., 2002). These concentrations are a function of the amount of detrital and Fe–Mn hydrogenous components (Th), and redox state (U), in the sediment (Plank and Langmuir, 1998), and greatly vary in any given location and individual layer of sediment. It is not possible to uniquely quantify ^{4}He ingrowth over time for these wide variations. Instead, the global subducting sediment (GLOSS) average of 6.91 ppm Th and 1.68 ppm U, with Th/U = 4.1 (Plank and Langmuir, 1998) is considered here to represent the effects of ^{4}He accumulation in ancient subducted sediment. Dehydration and heating during subduction is thought to remove some portion of U and Th from sediments from the slab although the exact amounts of removal continue to be debated (Elliott et al., 1997; Kelley et al., 2005; Kessel et al., 2005). The degree of U and Th removal will have a strong effect on the present-day He concentrations of ancient recycled sediment (Fig. 9). In the models presented
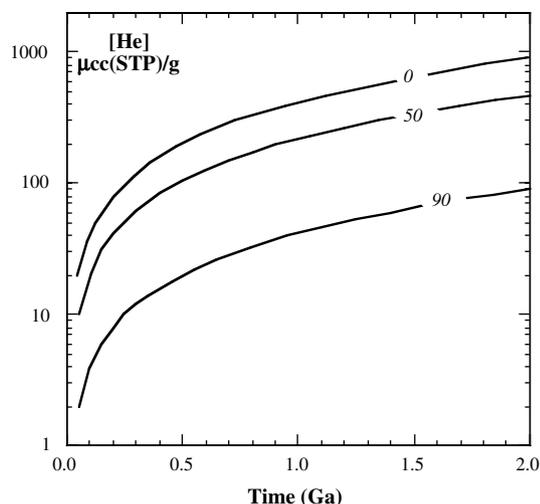
Fig. 9. The [He] in μcc(STP)/g of ancient recycled sediment, that is aged from 0 to 2 Ga, calculated using initial ^{3}He/^{4}He of 0.01 Ra, U abundances, and Th/U listed in Table 4. The curves represent 0%, 50%, and 90% loss of U and Th during subduction processes. Subsequent closed-system ingrowth of ^{4}He is calculated following these events.

here, the effects of 50% removal of U and Th are considered as an intermediate value resulting from removal during slab dehydration. It is also assumed that all of the He in sediment, irrespective of a meteoritic or endogenous origin, is outgassed during subduction (Hiyagon, 1994; Porcelli and Ballentine, 2002), such that the ^{3}He/^{4}He of the residual slab sediment is initially very low—a value of 0.01 Ra is assumed here because it adequately approximates the radiogenic ^{3}He/^{4}He production ratio.

4.2.2. Os constraints

The Os concentrations and isotopic compositions for present-day PM are well constrained and are used for the primitive mantle component present in the plume (Table 4; Meisel et al., 2001; Morgan et al., 2001; Brandon et al., 2006). The IDDM component represents a source with a slightly lower long-term Re/Os resulting from melt removal and loss of slightly incompatible Re relative to Os in the convecting mantle, consistent with the outgassing He model of Class and Goldstein (2005). The isotopic compositions for variably aged basalt and sediment components used in the models are based on mafic granulites and eclogites, representing dehydrated mafic slab material in subduction zones (Becker, 2000), and average reduced ocean floor sediment (Ravizza and Pyle, 1997; Brandon et al., 1999). These are evolved to present-day values using the average published Re and Os concentrations (Ravizza and Pyle, 1997; Brandon et al., 1999; Becker, 2000). Platinum, Re and Os are likely removed from slabs during subduction processes (Brandon et al., 1996; Brandon et al., 1999; McInnes et al., 1999; Becker, 2000; Becker et al., 2001; Becker et al., 2004; Sun et al., 2004). Therefore, the amount of ancient recycled crust of different ages required in a mixture with PM to create a hybrid component will increase proportionally to the amount of removal of Re and Os. In the case of the basalt

portion of the slab, the concentrations of mafic granulites and eclogites are considered to be those following removal during subduction processes. In the case of sediments in slabs, the effects of subduction zone processing on these elements is at present unknown. The composition of reduced sediments were chosen because of their relatively large concentrations of Re and Os (Table 4) compared to other ocean sediments, such that very small amounts of this material produce a strong increase in ^{187}Os/^{188}Os when added to PM to create the hybrid component.

4.2.3. Os–He isotope models

The results of the models for mixing of PM having 37 Ra and IDDM components having 37, 50.9, and 72.5 Ra (Table 4), with ancient recycled crust (ARC) are displayed in Fig. 10. The aim of this modeling is to produce a hybrid source having ^{3}He/^{4}He of $\geqslant 25$ Ra and ^{187}Os/^{188}Os $\geqslant 0.1381$, the maximum values for the Iceland neovolcanic zones lavas. The range of compositions for the hybrid source, when mixed with an upper mantle source having ^{3}He/^{4}He of $\leqslant 9$ Ra and ^{187}Os/^{188}Os $\leqslant 0.1297$, should produce compositions that fall within the shaded areas that extend beyond the upper end of the positive correlation of the Iceland picrites (Fig. 10). The He compositions used for the crustal end-members in these models are for a basalt that has undergone 99% outgassing during subduction, and for completely outgassed sediment that has 50% U and Th contents relative to GLOSS as a result of loss during subduction processes as discussed above.

Mixing curves between PM (Table 4) and three different ARC compositions, consisting of basalt, sediment, and 95 basalt:5 sediment, for 250 Ma and 2 Ga crust are shown (Fig. 10a). The shapes of the curves for different aged ARC of different compositions are generally the same. This is because the amounts of ^{4}He and ^{187}Os produced, which control the concentrations of He and Os in this crust, are proportional to the age of the crust having the same $(U + Th)/^3$He and Re/Os ratios (Table 4). Hence, the curves are generally independent of the age, only the proportions of the two end-members will be different for variable aged crust being mixed with PM. This conclusion also holds for other crustal materials unless the Re/Os ratios, and the concentrations of U and Th which affect the ^{4}He production rate, are strongly different.

All of these hybrid sources, where PM is mixed with variable amounts of basalt and sediment of different ages, could be potential end-members that when mixed with MORB mantle could produce the positive correlation between ^{187}Os/^{188}Os and ^{3}He/^{4}He. However, for all ARC compositions, younger ages require larger amounts of this component.

Mixing curves between different ARC compositions and IDDM having ages of 750 Ma, 1 Ga, and 1.5 Ga are shown (Fig. 10b). In the models, it is assumed that any ancient recycled crust in the hybrid mixture is equal to or older than the IDDM formation age. This is a logical approach because isolation of any mantle package consisting of a hybrid mixture of peridotite that underwent partial melting in the upper mantle with subsequent drawdown via convection (Porcelli, 2007), presumably will contain crust of the
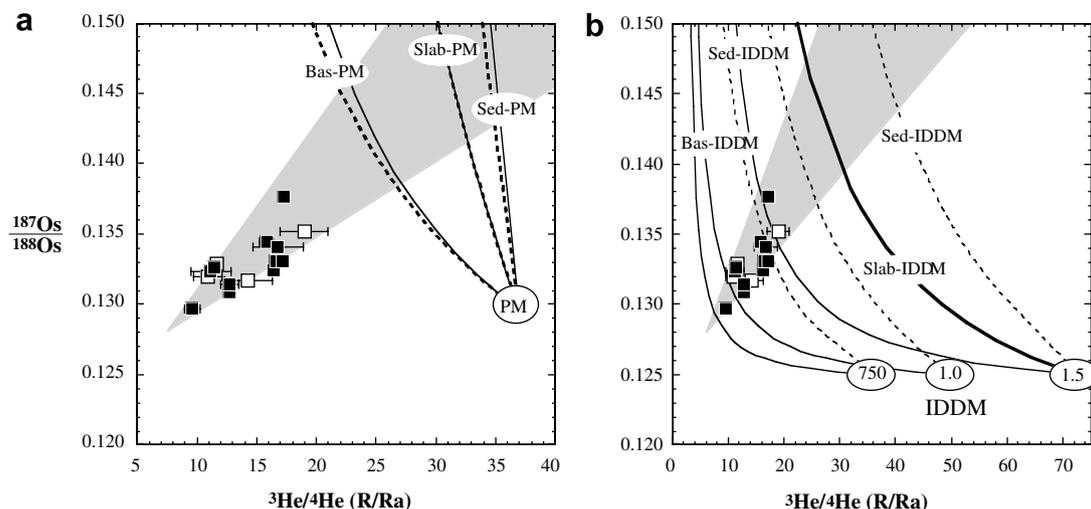
Fig. 10. (a) ^{3}He/^{4}He–^{187}Os/^{188}Os mixing models for a primitive mantle (PM) having ^{187}Os/^{188}Os = 0.1296 and ^{3}He/^{4}He = 37 Ra, with 250 Ma (dashed lines) and 2 Ga crustal (solid lines) compositions evolved to the present where Bas, basalt; Sed, sediment; Slab, 95 basalt:5 sediment. The Iceland picrite data are shown with symbols as in Fig. 5. See Table 4 for end-member compositions modeled and for hybrid slab–mantle components derived from the mixes. The shaded area is the region where mixing lines between a hybrid component with high ^{187}Os/^{188}Os and ^{3}He/^{4}He that is itself a mixture between PM and slab, and an upper mantle with low ^{187}Os/^{188}Os and ^{3}He/^{4}He will lie in order to plot along the trend for the Iceland picrite data. (b) ^{3}He/^{4}He–^{187}Os/^{188}Os mixing models for an incompletely degassed depleted mantle source (IDDM) of Class and Goldstein (2005) having ^{187}Os/^{188}Os = 0.1250 and formed at 750 Ma, 1.0 Ga, and 1.5 Ga with present-day ^{3}He/^{4}He = 37, 51, and 72 Ra, respectively. The age of the crustal components in the mixtures are 1 Ga for IDDM = 750 and 1.0 Ga, and 2 Ga for IDDM = 1.5 Ga. The thin solid lines are for mixing between recycled basalt and IDDM, the dashed lines for mixing between sediment and IDDM, and the thick solid line for mixing between slab and IDDM for 1.5 Ga only. See text for additional discussion.

same age or older, the latter resulting from a time lag between its formation at a mid-ocean ridge, until the time of subduction and entrainment within mantle. Hence, ancient recycled crust (ARC) ages of less than 1 Ga are not considered in these models generated for IDDM compositions. Because of the low concentrations of He in IDDM compared to the different aged recycled materials (Table 4), the mixing curves for IDDM with formation ages of 750 Ma to 1.5 Ga, show strong decreases from high ^{3}He/^{4}He with little change in ^{187}Os/^{188}Os, until ^{3}He/^{4}He values of 10 Ra or less are obtained. These curves do not produce viable hybrid compositions, with two exceptions. (1) Mixtures between pure sediment with 1.0 and 1.5 Ga IDDM falls within the desired region. This would require that the recycled material within the Iceland plume be predominantly sediment with little or no basalt, inconsistent with evidence from lithophile trace element and isotope compositions of Iceland lavas (Chauvel and Hemond, 2000; Thirlwall et al., 2004). (2) A 1.5 Ga IDDM having ^{3}He/^{4}He = 72.5 Ra, when mixed with a slab having proportions of 95 basalt:5 sediment a viable hybrid plume composition. These systematics show that if the high ^{3}He/^{4}He mantle in the Iceland plume source was related to partial melting that created continental crust in the past (Parman, 2007), then a formation age of 1.5 Ga or older is more realistic than younger ages. They also imply that this mantle has a much higher ^{3}He/^{4}He than any basalt or fluids that were ultimately derived from beneath the present-day Iceland region.

Formation of the hybrid components requires greater proportions of younger crust than older crust. It is possible

to estimate the amount of crust of a given age that is contained in a hybrid PM or IDDM source, which then mixes with the recent MORB mantle to generate the maximum ^{187}Os/^{188}Os of 0.1381 in the Iceland picrites (Fig. 11). In the case of a wholly basalt crust, the amount necessary
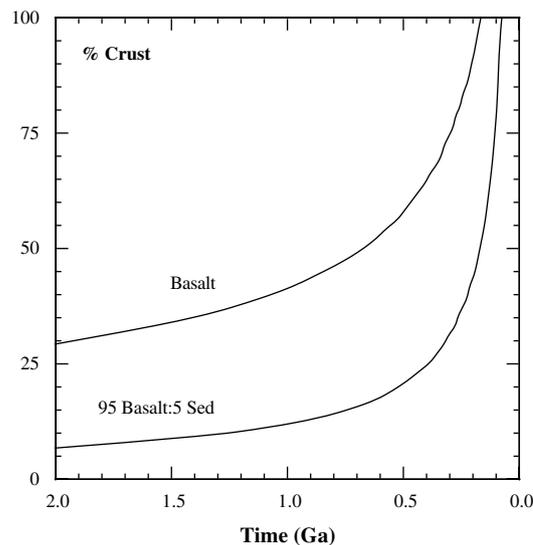

Fig. 11. The percent crust versus time of formation of crust, necessary in a mixture of hybrid mantle with MORB mantle to obtain the maximum value of ^{187}Os/^{188}Os for the Iceland picrites of 0.1381. End-member compositions used to model the evolution of the crustal sources and the mixtures are listed in Table 4.

within this mixture would range from ~30% for 2 Ga, to ~82% for 250 Ma. Such large amounts of basalt present in the mantle during partial melting are unlikely to produce primitive high MgO melts that are parental to picrites (Norman and Garcia, 1999). When a small amount of sediment is present, in the proportion of 95% basalt:5% sediment, the amount of crust required is significantly reduced, to 7% for 2 Ga ARC and to ~37% for 250 Ma ARC (Fig. 11). If the ARC containing 5% sediment is younger than 250 Ma, an even greater proportion is required in mixture. This is unviable from a petrologic standpoint. Hence, if the enrichments observed in the Iceland picrites result from having ARC in the mantle source, then these models show that the Os–He isotope relationships are not consistent with recycled crust as young as 170 Ma as previously proposed (Thirlwall et al., 2004). This is clearly apparent for a mixture containing IDDM, where the Os–He relationships shown in Fig. 10b indicate formation ages of >1.0 Ga and presumably constrain the age of the ARC to also be of that age or older. Hence, these enrichments become most easily generated from a mantle source with 1 Ga or older ARC, consistent with the constraints from Pb isotopic compositions of Iceland neovolcanic zone lavas modeled by Kokfelt et al. (2006), where less than 20% of a crust composed largely of basalt plus a small amount of sediment is present (Fig. 11). Such proportions of crust in the mantle source of oceanic island basalts, or mixing proportions between melts derived from such sources, is consistent with a wide spectrum of geochemical data (e.g., Lassiter and Hauri, 1998; Kogiso et al., 2004).

In summary, these models demonstrate that the mechanisms that could produce the Os–He systematics for the Iceland picrites are twofold. First, a hybrid mantle must exist from the juxtaposition of 1 Ga or older recycled crust and primitive mantle, or from melts derived from these sources. This hybrid mantle has radiogenic $^{187}Os/^{188}Os$ relative to MORB mantle or primitive mantle, but has elevated $^{3}He/^{4}He$. Mixing models incorporating a range of reasonable parameters for these materials can produce such a hybrid mantle source. Importantly, the most favorable models to explain Os–He systematics are those where both mafic material and small amounts of sediment from an ancient recycled slab are present in the Iceland mantle source. Second, this hybrid source must be physically separated from the MORB mantle in order to maintain its distinct geochemical characteristics over time. When the hybrid source is mixed with the MORB mantle, a quasi-linear array for $^{187}Os/^{188}Os$–$^{3}He/^{4}He$ as observed in the Iceland picrites is produced (Fig. 5a).

4.3. He isotope evidence for a compositionally evolving Iceland plume over 60 Ma?

The origin of the high $^{3}He/^{4}He$ signature observed in oceanic lavas is under considerable debate. Most proposed models for high $^{3}He/^{4}He$ range from an undegassed primordial source to a more outgassed source that has been isolated relative to the convecting upper mantle during the later stages Earth history (Class and Goldstein, 2005; Parman, 2007; Porcelli, 2007). In the case of a primordial

source, this ^{3}He source may be the outer core (Porcelli and Halliday, 2001) or the lower mantle (Kurz et al., 1982). The alternative models propose that isolated materials of high $^{3}He/^{4}He$ are present throughout the convecting upper mantle (Anderson, 2000; Coltice and Ricard, 2002; Meibom and Anderson, 2004; Meibom et al., 2005). These materials could be strongly melt depleted mantle blobs on a sub-kilometer scale that consist primarily of olivine (Meibom et al., 2005). A similar explanation involves harzburgitic ancient subcontinental lithosphere residing under cratons. Both of these materials would have lost U and Th through melt depletion in the past resulting in less ^{4}He ingrowth relative to the MORB mantle. Helium has a moderately high solubility in olivine; melt-depleted olivine-rich mantle might preserve a high $^{3}He/^{4}He$ signal if He behaves more compatibly than U and Th during partial melting (Graham et al., 1990; Parman et al., 2005).

The data for lavas from the Iceland magmatic system help constrain the origin of the high $^{3}He/^{4}He$ source in the context of such proposed models for oceanic basalts. As shown above, in order to explain the Os–He isotope systematics, the source of high $^{3}He/^{4}He$ first mixes with mantle that contains ancient recycled crust to create a hybrid source. Only after such a process has occurred, can the hybrid source then mix with the present-day MORB mantle. These conditions are inconsistent with models where all observed geochemical heterogeneities are juxtaposed in the upper mantle (i.e., a statistical upper mantle assemblage—SUMA, Meibom and Anderson, 2004; Meibom et al., 2005). Given the widely variable parameters of Os and He concentrations and isotopic compositions in mantle and crustal materials, SUMA-type models instead predict a wider array of scattering that is not observed, rather than the well-defined array for the Iceland picrite data (Fig. 5a). The high $^{3}He/^{4}He$ source therefore cannot have a direct physical relationship with the convecting MORB mantle over extended timescales and must exist in a region where recycled lithosphere/crustal material can be mixed in without contribution from the MORB mantle. A similar inference was made based on the negative correlation of low $\delta^{18}O$ with high $^{3}He/^{4}He$ observed in lavas from the neovolcanic zones in Iceland and the Reykjanes ridge (Thirlwall et al., 2006). Further support that the geochemical variability of Iceland magmatism reflects an origin from a deep mantle plume isolated from the present-day convecting MORB mantle may be inferred from the primordial Ne isotopic compositions in neovolcanic zone lavas (Dixon et al., 2000; Moreira et al., 2001). These arguments appear to eliminate models for volcanism in Iceland solely involving the upper mantle or lithosphere with no involvement of a deep, convectively isolated lower mantle source (Anderson, 2000; Foulger and Pearson, 2001; Meibom and Anderson, 2004; Foulger et al., 2005; Meibom et al., 2005). Whether the high $^{3}He/^{4}He$ originates from the lowermost mantle, as IDDM that was convected down (Porcelli, 2007), or PM, or from the core is uncertain. Coupled enrichments for $^{186}Os/^{188}Os$ and $^{187}Os/^{188}Os$ correlated with $^{3}He/^{4}He$ in Hawaiian picrites (Brandon et al., 1999) could be explained by primordial He derived from the core (e.g., Porcelli and Halliday,

2001). However, the Iceland picrites in this study show no enrichments in $^{186}Os/^{188}Os$ and do not support an origin of primordial He from the core unless the mechanisms
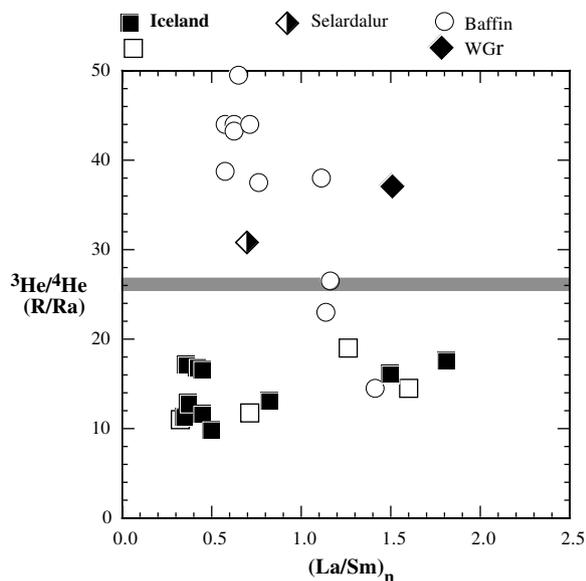

Fig. 12. $(La/Sm)_n$–$^3He/^4He$ for lavas from the Iceland plume from 61 Ma to present. Iceland picrite symbols as in Fig. 5. The 61 Ma Baffin Island picrites are from Stuart et al. (2003). The $(La/Sm)_n$ ratio of the least crustally contaminated picrite sample from the 61 Ma Vaigat Formation of West Greenland (Lightfoot et al., 1997) is combined with the highest $^3He/^4He$ value from a picrite from the same locale on Nuussuaq Peninsula (Graham et al., 1998). A late Tertiary lava from Selardalur (⩽14.9 Ma) in NW Iceland is from Harrison et al. (1999).

that impart outer core Os and He signatures to the lowermost mantle are not always coupled. Additional work is obviously required to further explore the origin of the deep high $^3He/^4He$ source.

A high $^3He/^4He$ source has been identified in the Iceland magmatic system since 60 Ma. A late Tertiary lava from Selardalur (⩽14.9 Ma) in NW Iceland has $^3He/^4He = 37$ Ra, 61 Ma picrites from the Vaigat Formation in West Greenland have $^3He/^4He$ of up to 31 Ra, and 61 Ma picrites from Baffin Island that are correlative with those from West Greenland have $^3He/^4He$ of up to 49.5 Ra (Graham et al., 1998; Hilton et al., 1999; Stuart et al., 2003). East Greenland picrites erupted from the Iceland plume at 58 Ma have $^3He/^4He$ of up to 20 Ra, but likely have been lowered via crustal contamination (Marty et al., 1998).

The high $^3He/^4He$ in these older lavas is not reflected to the same degree in the neovolcanic zones of Iceland. This is exemplified by the Iceland picrites in this study that have distinct isotope and trace element characteristics relative to those for the earlier lavas (Figs. 12 and 13). For example the combined $^3He/^4He$, ε_{Nd} (i.e., $^{143}Nd/^{144}Nd$ normalized to chondrite uniform reservoir—CHUR), ΔNb, and $(La/Sm)_n$ systematics for these lavas show that a strong compositional gap exists between the samples with high $^3He/^4He$ in the older lavas and the neovolcanic zone lavas. The Nd–He isotope systematics in particular, show different relationships for the older Iceland plume lavas compared to lavas from the neovolcanic zones (Fig. 13a). The older lavas have experienced some mixing between Precambrian Greenland crust and a mantle plume component of high $^3He/^4He$ (Marty et al., 1998). These observations, combined with the fact that all neovolcanic zone lavas have $^3He/^4He < 27$ Ra, suggest that a fundamental change

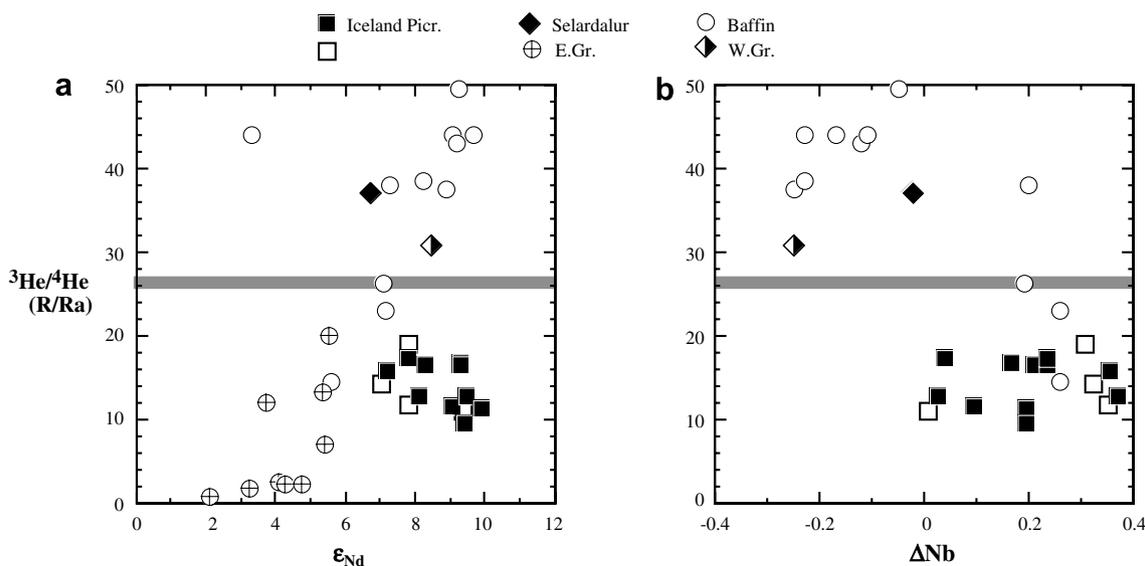Fig. 13. (a) ε_{Nd}–$^3He/^4He$ for lavas from the Iceland plume from 61 Ma to present. Additional picrite samples from the 58 Ma East Greenland are from Marty et al. (1998). The $^{143}Nd/^{144}Nd$ of the samples older than present have been corrected to the present by first calculating their Sm/Nd ratios for their sources relative to the CHUR value for each age (present-day CHUR $^{143}Nd/^{144}Nd = 0.512638$, $^{147}Sm/^{144}Nd = 0.1967$) evolving the $^{143}Nd/^{144}Nd$ to present using the calculated Sm/Nd of the sources. $\varepsilon_{Nd} = [(^{143}Nd/^{144}Nd_{sample}/^{143}Nd/^{144}Nd_{CHUR}) - 1] \times 10^4$. (b) ΔNb–$^3He/^4He$ for lavas from the Iceland plume from 61 Ma to present. $\Delta Nb = 1/75 + \log(Nb/Y) - 1.92\log(Zr/Y)$ (Fitton et al., 1997). Iceland picrite symbols as in Fig. 5.

occurred in the character of the Iceland plume source during the past 60 million years. The ^{3}He/^{4}He of ~50 Ra in the older picrites with high ε_{Nd} and subchondritic $(La/Sm)_n$ suggests a source more depleted in U + Th and light rare earth elements. At the onset of plume head impingement under Greenland, recycled crust/lithosphere components were therefore either not present in significant amounts, or were not effectively sampled within the upwelling plume. In more recent times and with further upwelling, recycled lithosphere entrained within the plume was more prevalent, as reflected by the mixture of the hybrid component plus MORB mantle that produces the Os–He isotope systematics of the Iceland picrites. Therefore, the distinct high ^{3}He/^{4}He compositions of the different aged Iceland magmatic rocks are interpreted here as a manifestation of the same, deep-mantle source of He, and the observed compositional variations are related to changes in the dynamics and melting of the plume system over time.

5. CONCLUSIONS

The Os and He isotopes of Iceland picrites provide important insights into the Iceland plume system from 60 Ma to present. High-precision ^{186}Os/^{188}Os–^{187}Os/^{188}Os data for these picrites do not display coupled enrichments observed in other suites including Hawaiian picrites, Gorgona komatiites, and a sample from the Siberian plume system. Instead the Iceland picrites show uniform ^{186}Os/^{188}Os with an average of 0.1198375 ± 32, similar to the estimated present-day primitive mantle value of 0.1198398 ± 16. The lack of variation in ^{186}Os/^{188}Os is coupled with a range of variation in ^{187}Os/^{188}Os from 0.1297 to 0.1381. These systematics are reasonably explained by addition of 1–2 Ga recycled crust into the source of the Iceland plume. This is consistent with lithophile isotope and elemental evidence from these picrites and other neovolcanic zone lavas for a recycled crust contribution to the Iceland mantle plume. These inferences demonstrate that addition of ancient recycled crust into the source regions of plumes does not result in coupled enrichments of ^{186}Os/^{188}Os and ^{187}Os/^{188}Os found in other plume systems studied previously. If so, the coupled enrichments result by another mechanism, such as injection of evolved outer core metal into mantle plume sources at the core–mantle boundary. This process may be localized to such an extent that not all plume systems will show evidence of core–mantle interaction.

The Iceland picrites show a positive correlation between ^{187}Os/^{188}Os from 0.1297 to 0.1381 and ^{3}He/^{4}He from 9.6 to 19 Ra, respectively. The most favorable models that explain the origin of this variation are two types. In the first model, recycled crust older than 1 Ga is initially mixed with primitive mantle (either as solids or as melts derived from these sources), generating a hybrid mantle source with radiogenic ^{187}Os/^{188}Os but with elevated ^{3}He/^{4}He. The relationships between ^{187}Os/^{188}Os and ^{3}He/^{4}He with solar Ne isotopic compositions of some Iceland lavas, are consistent with a deep mantle origin of the ^{3}He/^{4}He mantle component, where juxtaposition of an early formed layer with high ^{3}He/^{4}He and younger recycled material may occur at the core-mantle boundary over Earth history (Tolstikhin and Hofmann, 2005). Successful mixing models to create the hybrid plume source show that the primordial He source could have ^{3}He/^{4}He as low as 37 Ra, similar to the maximum value measured in recent Iceland lavas.

In the second model, an incompletely degassed depleted mantle source (Class and Goldstein, 2005) that was isolated at least 1.0–1.5 Ga in the past, and consequently evolving to the present with an elevated ^{3}He/^{4}He relative to the MORB mantle is mixed with ancient recycled crust to create a hybrid mantle source. If this model is valid, the present-day ^{3}He/^{4}He of this source must be on the order of 50–70 Ra, much greater than the ^{3}He/^{4}He measured in recent Iceland lavas but similar to those erupted from the Iceland plume at 60 Ma. This model also requires that the ancient recycled crust contributing to Iceland magmatism is of the same age or older, and would eliminate models supporting a Phanerozoic age for the recycled crust contributing to Iceland magmatism. The primary drawback to such a model is that it must be reconciled in the context of the observed solar Ne isotopic compositions present in some high ^{3}He/^{4}He Iceland lavas.

Whichever of the two models for the high ^{3}He/^{4}He source is correct, the ancient recycled crust must be juxtaposed with the high ^{3}He/^{4}He mantle and both are physically separated from the convecting MORB mantle. Mixing with MORB mantle subsequently produces the quasi-linear array for ^{187}Os/^{188}Os–^{3}He/^{4}He observed in the Iceland picrites.

The relationships between He–Nd–Os isotopes and lithophile element concentrations have changed during the eruptive history of the Iceland plume. At 60 Ma, lavas erupted from the ancestral plume head which impinged upon the Greenland craton appear to have sampled little or no recycled crust within the plume. Upon continued upwelling from the deep mantle, ancient recycled material was brought into the zone of melting under Iceland, probably during the last 15 Ma.

Finally, the modeling presented here to explain the origin of the positive correlation between ^{187}Os/^{188}Os and ^{3}He/^{4}He demonstrates the Iceland lava He isotopic compositions do not result from simple melt depletion histories in their mantle sources. Instead their He isotopic compositions result from complex mixtures of materials formed at different times. Hence, the He isotopic compositions of ocean lavas should not be used at face value to create coupled models for the timing of mantle melting and crustal growth (e.g., Parman, 2007).

APPENDIX A

Bulk-rock element concentrations obtained from X-ray fluorescence

Sample	SiO_2	TiO_2	Al_2O_3	Fe_2O_3	MnO	MgO	CaO	Na_2O	K_2O	P_2O5	Cr_2O_3	Cu	Ni	V	LOI	Total
ICE-0	46.61	0.414	11.12	10.02	0.160	20.11	10.45	1.10	0.03	0.028	3188	154	749	176	—	100.47
ICE-2	45.94	0.374	11.76	9.35	0.147	20.72	10.39	1.16	0.01	0.025	3448	111	750	156	—	100.32
ICE-3	45.59	1.232	11.71	12.35	0.186	18.00	9.25	1.55	0.19	0.158	2042	210	588	214	—	100.52
ICE-4a	44.36	0.544	8.95	10.99	0.164	25.27	8.71	0.99	0.02	0.027	2343	147	937	159	—	100.38
ICE-4b	44.56	0.576	9.51	10.90	0.163	23.85	9.24	1.19	0.02	0.025	2222	101	866	176	—	100.37
ICE-5	45.54	0.618	12.20	10.71	0.164	18.76	11.07	1.19	0.02	0.026	1706	172	602	189	—	100.56
ICE-6	47.38	0.824	14.83	10.59	0.170	12.48	12.10	1.71	0.05	0.061	1191	231	332	226	—	100.39
ICE-8a	46.48	1.721	11.36	12.47	0.186	15.62	7.92	2.10	0.38	0.210	1779	110	608	252	1.31	100.03
ICE-8b	46.50	1.453	10.14	12.21	0.183	19.27	7.16	1.96	0.24	0.186	2447	169	843	212	0.68	100.35
ICE-9a	47.68	2.004	11.76	12.64	0.179	12.96	9.11	2.21	0.44	0.222	1345	248	464	298	0.61	100.05
ICE-10	47.30	0.858	14.79	10.58	0.168	12.33	12.15	1.79	0.06	0.058	1283	183	311	227	—	100.28
ICE-11	46.22	0.392	14.28	9.15	0.145	17.38	11.17	1.42	0.02	0.024	2285	219	516	157	—	100.52
DMF-9101	44.72	0.529	10.55	10.81	0.164	22.37	9.81	1.11	0.02	0.021	2004	177	1011	169	—	100.44
9805	44.07	0.214	9.66	9.30	0.139	28.47	7.69	0.80	0.01	0.016	4370	75	1205	101	—	100.94
9806	46.72	0.517	15.24	9.20	0.146	15.17	11.76	1.43	0.04	0.037	1889	196	432	170	—	100.53
9809	44.59	0.331	10.45	9.96	0.151	24.78	8.61	0.93	0.01	0.020	3510	174	990	146	—	100.31
9810	46.99	1.478	14.47	12.77	0.194	10.70	11.09	2.08	0.16	0.138	758	204	250	294	—	100.22
9812	46.93	0.460	14.46	9.09	0.148	15.95	11.71	1.45	0.02	0.027	1743	217	517	172	—	100.51
9815	47.93	1.473	14.72	11.96	0.187	9.47	11.91	2.19	0.18	0.176	769	256	185	298	—	100.35

Major elements are listed in weight percent, Cr_2O_3, Cu, Ni, and V are in parts per million. LOI—lost on ignition.

REFERENCES

Anders E. and Grevesse N. (1989) Abundances of the elements: meteoritic and solar. *Geochim. Cosmochim. Acta* **53**, 197–214.

Anderson D. (2000) The statistics of helium isotopes along the global spreading ridge system and the Central Limit Theorem. *Geophys. Res. Lett.* **27**, 2401–2404.

Baker J. A. and Jensen K. K. (2004) Coupled [186]Os–[187]Os enrichments in the Earth's mantle—core–mantle interaction or recycling of ferromanganese crusts and nodules? *Earth Planet. Sci. Lett.* **220**, 277–286.

Ballentine C. J., Marty B., Lollar B. S. and Cassidy M. (2005) Neon isotopes constrain convection and volatile origin in the Earth's mantle. *Nature* **433**, 33–38.

Becker H. (2000) Re–Os fractionation in eclogites and blueschists and the implications for recycling of oceanic crust into the mantle. *Earth Planet. Sci. Lett.* **177**, 287–300.

Becker H., Carlson R. W. and Shirey S. B. (2004) Slab-derived osmium and isotopic disequilibrium in garnet pyroxenites from a Paleozoic convergent plate margin (lower Austria). *Chem. Geol.* **208**, 141–156.

Becker H., Jochum K. P. and Carlson R. W. (2000) Trace element fractionation during dehydration of eclogites from high-pressure terranes and the implications for element fluxes in subduction zones. *Chem. Geol.* **163**, 65–99.

Becker H., Shirey S. B. and Carlson R. W. (2001) Effects of melt percolation on the Re–Os systematics of peridotites from a Paleozoic convergent plate margin. *Earth Planet. Sci. Lett.* **188**, 107–121.

Begemann F., Ludwig K. R., Lugmair G. W., Min K., Nyquist L. E., Patchett P. J., Renne P. R., Shih C.-Y., Villa I. M. and Walker R. J. (2001) Call for an improved set of decay constants for geochronological use. *Geochim. Cosmochim. Acta* **65**, 111–121.

Bennett V. C., Esat T. M. and Norman M. D. (1996) Two mantle plume components in Hawaiian picrites inferred from correlated Os–Pb isotopes. *Nature* **381**, 221–224.

Brandon A. D., Becker H., Carlson R. W. and Shirey S. B. (1999) Isotopic constraints on time scales and mechanisms of slab material transport in the mantle wedge: evidence from the Simcoe mantle xenoliths, Washington, USA. *Chem. Geol.* **160**, 387–407.

Brandon A. D., Creaser R. A., Shirey S. B. and Carlson R. W. (1996) Osmium recycling in subduction zones. *Science* **272**, 861–864.

Brandon A. D., Graham D. and Gautason B. (2001) [187]Os–[186]Os and He isotope systematics of Iceland picrites. *Eos, Trans. Am. Geophys. Un.* **82**(Suppl.), F1306.

Brandon A. D., Humayun M. and Puchtel I. S. (2005a) Re–Os isotopic systematics and platinum group element composition of the Tagish Lake carbonaceous chondrite. *Geochim. Cosmochim. Acta* **69**, 1619–1631.

Brandon A. D., Humayun M., Puchtel I. S., Leya I. and Zolensky M. (2005b) Osmium isotope evidence for an s-process carrier in primitive chondrites. *Science* **309**, 1233–1236.

Brandon A. D., Norman M. D., Walker R. J. and Morgan J. W. (1999) [186]Os–[187]Os systematics of Hawaiian picrites. *Earth Planet. Sci. Lett.* **174**, 25–42.

Brandon A. D., Snow J. E., Walker R. J., Morgan J. W. and Mock T. D. (2000) [190]Pt–[186]Os and [187]Re-[187]Os systematics of abyssal peridotites. *Earth Planet. Sci. Lett.* **177**, 319–335.

Brandon A. D. and Walker R. J. (2005) The debate over core-mantle interaction. *Earth Planet. Sci. Lett.* **232**, 211–225.

Brandon A. D., Walker R. J., Morgan J. W. and Norman M. D. and Prichard H. M. (1998) Coupled [186]Os and [187]Os evidence for core-mantle interaction. *Science* **280**, 1570–1573.

Brandon A. D., Walker R. J. and Puchtel I. S. (2006) Platinum–osmium isotope evolution of the Earth's mantle: constraints from chondrites and Os-rich alloys. *Geochim. Cosmochim. Acta* **70**, 2093–2103.

Brandon A. D., Walker R. J., Puchtel I. S., Becker H., Humayun M. and Revillon S. (2003) [186]Os–[187]Os systematics of Gorgona Island komatiites: implications for early growth of the inner core. *Earth Planet. Sci. Lett.* **206**, 411–426.

Breddam K., Kurz M. D. and Storey M. (2000) Mapping out the conduit of the Iceland mantle plume with helium isotopes. *Earth Planet. Sci. Lett.* **176**, 45–55.

Chabot N. L. and Jones J. H. (2003) The parameterization of solid metal–liquid metal partitioning of siderophile elements. *Meteorit. Planet. Sci.* **38**, 1425–1436.

Chauvel C. and Hemond C. (2000) Melting of a complete section of recycled oceanic crust: trace element and Pb isotopic evidence from Iceland. *Gechem. Geophys. Geosys.* **1**, 1999GC000002.

Class C. and Goldstein S. L. (2005) Evolution of helium isotopes in the Earth's mantle. *Nature* **436**, 1107–1112.

Coltice N. and Ricard Y. (2002) On the origin of noble gases in mantle plumes. *Phil. Trans. R. Soc. Lond. A* **360**, 2633–2648.

Dixon E. T. (2003) Interpretation of helium and neon isotopic heterogeneity in Icelandic basalts. *Earth Planet. Sci. Lett.* **206**, 83–99.

Dixon E. T., Honda M., McDougall I., Campbell I. H. and Sigurdsson I. (2000) Preservation of near-solar neon isotopic ratios in Icelandic basalts. *Earth Planet. Sci. Lett.* **180**, 309–324.

Dodson A. and Brandon A. D. (1999) Radiogenic helium in xenoliths from Simcoe, Washington, USA: implications for metasomatic processes in the mantle wedge above subduction zones. *Chem. Geol.* **160**, 371–386.

Eiler J. M., Farley K. A. and Stolper E. M. (1998) Correlated helium and lead isotope variations in Hawaiian lavas. *Geochim. Cosmochim. Acta* **62**, 1977–1984.

Ellam R. M. and Stuart F. M. (2004) Coherent He–Nd–Sr isotope trends in high ^{3}He/^{4}He basalts: implications for a common reservoir, mantle heterogeneity and convection. *Earth Planet. Sci. Lett.* **228**, 511–523.

Elliott T., Plank T., Zindler A., White W. and Bourdon B. (1997) Element transport from slab to volcanic front at the Mariana arc. *J. Geophys. Res.* **102**, 14991–15019.

Fitton J. G., Saunders A. D., Norry M. J., Hardarson B. S. and Taylor R. N. (1997) Thermal and chemical structure of the Iceland plume. *Earth Planet. Sci. Lett.* **153**, 197–208.

Foulger G. R., Natland J. H. and Anderson D. L. (2005) A source for Icelandic magmas in remelted Iapetus crust. *J. Volcanol. Geotherm. Res.* **141**, 23–44.

Foulger G. R. and Pearson D. G. (2001) Is Iceland underlain by a plume in the lower mantle. Seismology and helium isotopes. *Geophys. J. Int.* **145**, F1–F5.

Graham D. (2002) Noble gas isotope geochemistry of mid-ocean ride and ocean island basalts: characterization of mantle source reservoirs. In *Noble Gases in Geochemistry and Cosmochemistry*, vol. 47 (eds. D. Porcelli, C. J. Ballentine and R. Wieler). Min. Soc. Am., Washington, pp. 247–317.

Graham D. (2005) Neon illuminates the mantle. *Nature* **433**, 25–26.

Graham D., Larsen L. M., Hanan B. B., Storey M., Pedersen A. K. and Lupton J. E. (1998) Helium isotope composition of the early Iceland mantle plume inferred from Tertiary picrites of West Greenland. *Earth Planet. Sci. Lett.* **160**, 241–255.

Graham D., Lupton J., Albarade F. and Condomines M. (1990) Extreme temporal homogeneity of helium isotope at Piton de La Fournaise, Reunion Island. *Nature* **347**, 545–548.

Hanan B. B., Blichert-Toft J., Kingsley R. and Schilling J. G. (2000) Depleted Iceland mantle plume geochemical signature: Artifact of multicomponent mixing? *Geochem. Geophys. Geosys.* **1**, 1999GC000009.

Hanan B. B. and Schilling J.-G. (1997) The dynamic evolution of the Iceland mantle plume: the lead isotope perspective. *Earth Planet. Sci. Lett.* **151**, 43–60.

Harrison D., Burnard P. and Turner G. (1999) Noble gas behaviour and composition in the mantle: constraints from the Iceland Plume. *Earth Planet. Sci. Lett.* **171**, 199–207.

Hart S. R., Blusztajn J., Dick H. J. B., Meyer P. S. and Muehlenbachs K. (1999) The fingerprint of seawater circulation in a 500-meter section of ocean crust gabbros. *Geochim. Cosmochim. Acta* **63**, 4059–4080.

Hauri E. H. (1996) Major-element variability in the Hawaiian mantle plume. *Nature* **382**, 415–419.

Hemond C., Arndt N. T., Lichtenstein U., Hofmann A. W., Askarsson N. and Steinthorsson S. (1993) The heterogeneous Iceland plume: Nd–Sr–O isotopes and trace element constraints. *J. Geophys. Res.* **98**, 15833–15850.

Hilton D. R., Gronvold K., Macpherson C. G. and Castillo P. (1999) Extreme ^{3}He/^{4}He ratios in northwest Iceland: constraining the common component in mantle plumes. *Earth Planet. Sci. Lett.* **173**, 53–60.

Hiyagon H. (1994) Retention of helium in subducted interplanetary dust particles—reply. *Science* **265**, 1893.

Hofmann A. W. (1988) Chemical differentiation of the Earth: the relationship between mantle, continental crust, and oceanic crust. *Earth Planet. Sci. Lett.* **90**, 297–314.

Hofmann A. W. and Jochum K. P. (1996) Source characteristics derived from very incompatible trace elements in Mauna Loa and Mauna Kea basalts, Hawaii Scientific Drilling Project. *J. Geophys. Res.* **101**, 11831–11839.

Humayun M., Puchtel I. S. and Brandon A. D. (2002) PGEs in Icelandic picrites. *Geochim. Cosmochim. Acta* **66**, S1, 12th Ann. Goldschmidt Conf., A347.

Humayun M., Qin L. and Norman M. (2004) Geochemical evidence for excess iron in the Hawaiian mantle: implications for mantle dynamics. *Science* **306**, 91–94.

Kelley K. A., Plank T., Farr L., Ludden J. and Staudigel H. (2005) Subduction cycling of U, Th, and Pb. *Earth Planet. Sci. Lett.* **234**, 369–383.

Kempton P. D., Fitton J. G., Saunders A. D., Nowell G. M., Taylor R. N., Hardarson B. S. and Pearson G. (2000) The Iceland plume in space and time: a Sr–Nd–Pb–Hf study of the North Atlantic rifted margin. *Earth Planet. Sci. Lett.* **177**, 255–271.

Kessel R., Schmidt M. W., Ulmer P. and Pettke T. (2005) Trace element signature of subduction-zone fluids, melts and supercritical liquids at 120–180 km depth. *Nature* **437**, 724–727.

Klinkhammer G. P. and Palmer M. R. (1991) Uranium in the oceans: where it goes and why. *Geochim. Cosmochim. Acta* **55**, 1799–1806.

Kogiso T., Hirschmann M. M. and Reiners P. W. (2004) Length scales of mantle heterogeneities and their relationship to ocean island basalt geochemistry. *Geochim. Cosmochim. Acta* **68**, 345–360.

Kokfelt T. F., Hoernle K., Hauff F., Fiebig J., Werner R. and Garbe-Shonberg D. (2006) Combined trace element and Pb–Nd–Sr–O isotope evidence for recycled oceanic crust (Upper and Lower) in the Iceland mantle. *J. Petrol.* **47**, 1673–1704.

Kurz M. D., Jenkins W. J. and Hart S. R. (1982) Helium isotopic systematics of oceanic islands and mantle heterogeneity. *Nature* **297**, 43–47.

Kurz M. D., Meyer P. S. and Sigurdsson H. (1985) Helium isotopic systematics within the neovolcanic zones of Iceland. *Earth Planet. Sci. Lett.* **74**, 291–305.

Lassiter J. C. and Hauri E. H. (1998) Osmium isotope variation in hawaiian lavas: evidence for recycled oceanic lithosphere in the Hawaiian plume. *Earth Planet. Sci. Lett.* **164**, 483–496.

Lauer H. V. and Jones J. H. (1998) Partitioning of Pt and Os between solid and liquid metal in the iron–nickel–sulfur system. *Proc. Lunar Planet. Sci Conf.* **XXIX**, 1796.

Lightfoot P. C., Hawkesworth C. J., Olshefsky K., Green T., Doherty W. and Keays R. R. (1997) Geochemistry of Tertiary tholeiites and picrites from Qeqetarssuaq (Disko Island) and

Nuussuaq, West Greenland with implications for the mineral potential of comagmatic intrusions. *Contrib. Mineral. Petrol.* **128**, 139–163.

Luais B., Telouk P. and Albarede F. (1997) Precise and accurate neodymium isotopic measurements by plasma-source mass spectrometry. *Geochim. Cosmochim. Acta* **61**, 4847–4854.

Macpherson C. G., Hilton D. R., Day J. M. D., Lowry D. and Gronvold K. (2005) High-^{3}He/^{4}He, depleted mantle and low-δ^{18}O, recycled lithosphere in the source of the central Iceland magmatism. *Earth Planet. Sci. Lett.* **233**, 411–427.

Marty B., Upton B. G. J. and Ellam R. M. (1998) Helium isotopes in early Tertiary basalts, northeast Greenland: evidence for 58 Ma plume activity in the North Atlantic-Iceland volcanic province. *Geology* **26**, 407–410.

McInnes B. I. A., McBride J. S., Evans N. J., Lambert D. D. and Andrew A. S. (1999) Osmium isotope constraints on ore metal recycling in subduction zones. *Science* **286**, 512–516.

Meibom A. and Anderson D. L. (2004) The statistical upper mantle assemblage. *Earth Planet. Sci. Lett.* **217**, 123–139.

Meibom A., Sleep N. H., Zahnle K. and Anderson D. L. (2005) Models for nobel gases in mantle geochemistry: Some observations and alternatives. In *Plates, plumes, and paradigms: Geol. Soc. Am. Spec. Paper*, vol. 388 (eds. G. R. Foulger, J. H. Natland, D. C. Presnall and D. L. Anderson). pp. 347–363.

Meisel T., Walker R. J., Irving A. J. and Lorand J.-P. (2001) Osmium isotopic compositions of mantle xenoliths: a global perspective. *Geochim. Cosmochim. Acta* **65**, 1311–1323.

Moreira M., Blustajn J., Curtice J., Hart S., Dick H. and Kurz M. (2003) He and Ne isotopes in oceanic crust: implications for noble gas recycling in the mantle. *Earth Planet. Sci. Lett.* **216**, 635–643.

Moreira M., Kunz J. and Allegre C. (2001) Solar neon in the Icelandic mantle: new evidence for an undegassed lower mantle. *Earth Planet. Sci. Lett.* **185**, 15–23.

Moreira M. and Sarda P. (2000) Noble gas constraints on degassing processes. *Earth Planet. Sci. Lett.* **176**, 375–386.

Morgan J. W., Horan M. F., Walker R. J. and Grossman J. N. (1995) Rhenium–osmium concentration and isotope systematics in group IIAB iron meteorites. *Geochim. Cosmochim. Acta* **59**, 2331–2344.

Morgan J. W., Walker R. J., Brandon A. D. and Horan M. F. (2001) Siderohile elements in the Earth's upper mantle and lunar breccias: data synthesis suggests manifestations of the same late influx. *Meteor. Planet. Sci.* **36**, 1257–1275.

Nielsen S. G., Rehkamper M., Norman M. D., Halliday A. N. and Harrison D. (2006) Thallium isotopic evidence for ferromanganese sediments in the mantle source of Hawaiian basalts. *Nature* **439**, 314–317.

Norman M. D. and Garcia M. O. (1999) Primitive magmas and source characteristics of the Hawaiian plume petrology and geochemistry of shield picrites. *Earth Planet. Sci. Lett.* **168**, 27–44.

Parman S. W. (2007) Helium isotopic evidence for episodic mantle melting and crustal growth. *Nature* **446**, 900–903.

Parman S. W., Kurz M. D., Hart S. R. and Grove T. L. (2005) Helium solubility in olivine and implications for high ^{3}He/^{4}He in ocean island basalts. *Nature* **437**, 1140–1143.

Plank T., Balzer V. and Carr M. (2002) Nicaraguan volcanoes record paleoceanographic changes accompanying closure of the Panama gateway. *Geology* **30**, 1087–1090.

Plank T. and Langmuir C. H. (1998) The chemical composition of subducting sediment and its consequences for the crust and mantle. *Chem. Geol.* **145**, 325–394.

Porcelli D. (2007) When crust is bred. *Nature* **446**, 863–864.

Porcelli D. and Ballentine C. J. (2002) Models for the distribution of terrestrial noble gases and evolution of the atmosphere. In *Noble Gases in Geochemistry and Cosmochemistry*, vol. 47 (eds. D. Porcelli, C. J. Ballentine and R. Wieler). Min. Soc. Am., Washington, pp. 411–480.

Porcelli D. and Halliday A. N. (2001) The core as a possible source of mantle helium. *Earth Planet. Sci. Lett.* **192**, 45–56.

Puchtel I. S., Brandon A. D. and Humayun M. (2004) Precise Pt–Re–Os isotope systematics of the mantle from 2.7 Ga komatiites. *Earth Planet. Sci. Lett.* **224**, 157–174.

Puchtel I. S., Brandon A. D., Humayun M. and Walker R. J. (2005) Evidence for the early differentiation of th core from Pt–Re–Os isotope systematics of 2.8-Ga komatiites. *Earth Planet. Sci. Lett.* **237**, 118–134.

Ravizza G. and Pyle D. (1997) PGE and Os isotopic analyses of single sample aliquots with NiS fire assay preconcentration. *Chem. Geol.* **141**, 251–268.

Salters V. J. M. and Stracke A. (2004) Composition of the depleted mantle. *Geochem. Geophys. Geosyst.* **5**, 2003GC000597.

Schersten A., Elliott T., Hawkesworth C. and Norman M. D. (2004) Tungsten isotope evidence that mantle plumes contain no contribution from the Earth's core. *Nature* **427**, 234–237.

Shirey S. B. and Walker R. J. (1998) The Re–Os isotope system in cosmochemistry and high-temperature geochemistry. *Ann. Rev. Earth Planet. Sci.* **26**, 423–500.

Skovgaard A. C., Storey M., Baker J., Blusztajn J. and Hart S. R. (2001) Osmium–oxygen isotope evidence for a recycled and strongly depleted component in the Iceland mantle plume. *Earth Planet. Sci. Lett.* **194**, 259–275.

Smith A. (2003) Critical evaluation of Re–Os and Pt–Os isotopic evidence on the origin of intraplate volcanism. *J. Geodyn.* **36**, 469–484.

Smoliar M. I., Walker R. J. and Morgan J. W. (1996) Re–Os ages of group IIA, IIIA, IVA, and IVB iron meteorites. *Science* **271**, 1099–1102.

Staudigel H., Plank T., White B. and Schmincke H.-U. (1996) Geochemical fluxes during seafloor alteration of the upper oceanic crust: DSDP sites 417–418. In *Subduction Top to Bottom. Geophysical Monograph. Bebout*, vol. 96 (eds. G. E. Bebout, D. W. Scholl, S. H. Kirby and J. P. Platt). American Geophysical Union, Washington, DC, pp. 19–38.

Stecher O., Carlson R. W. and Gunnarsson B. (1999) Torfajokull: a radiogenic end-member of the Iceland Pb-isotope array. *Earth Planet. Sci. Lett.* **165**, 117–127.

Stuart F. M., Lass-Evans S., Fitton J. G. and Ellam R. M. (2003) High ^{3}He/^{4}He ratios in picritic basalts from Baffin Island and the role of a mixed reservoir in mantle plumes. *Nature* **423**, 57–59.

Sun S. S. and McDonough W. F. (1989) Chemical and isotopic systematics of oceanic basalts; implications for mantle composition and processes. In *Magmatism in the Ocean Basins* (eds. A. D. Saunders and M. J. Norry). Geological Society of London, London, pp. 313–345.

Sun W., Bennett V. C. and Kamenetsky V. S. (2004) The mechanism of Re enrichment in arc magmas: evidence from Lau Basin basaltic glasses and primitive melt inclusions. *Earth Planet. Sci. Lett.* **222**, 101–114.

Taylor R. N., Thirlwall M. F., Murton B. J., Hilton D. R. and Gee M. A. M. (1997) Isotopic constrains on the influence of the Icelandic plume. *Earth Planet. Sci. Lett.* **148**, E1–E8.

Thirlwall M. F., Gee M. A. M., Lowry D., Mattey D. P., Murton B. J. and Taylor R. N. (2006) Low δ^{18}O in the Icelandic mantle and its origins: evidence from the Reykjanes ridge and Icelandic lavas. *Geochim. Cosmochim. Acta* **70**, 993–1019.

Thirlwall M. F., Gee M. A. M., Taylor R. N. and Murton B. J. (2004) Mantle components in Iceland and adjacent ridges

investigated using double-spike Pb isotope ratios. *Geochim. Cosmochim. Acta* **68**, 361–386.

Tolstikhin I. and Hofmann A. W. (2005) Early crust on top of the Earth's core. *Phys. Earth Planet. Int.* **148**, 109–130.

Walker D. (2000) Core participation in mantle geochemistry. *Geochim. Cosmochim. Acta* **64**, 2897–2911.

Walker R. J., Brandon A. D., Bird J. M., Piccoli P. M., McDonough W. F. and Ash R. D. (2005) ^{187}Os–^{186}Os systematics of Os–Ir–Ru alloy grains from southwestern Oregon. *Earth Planet. Sci. Lett.* **230**, 211–226.

Walker R. J., Morgan J. W., Beary E., Smoliar M. I., Czamanske G. K. and Horan M. F. (1997) Applications of the ^{190}Pt–^{186}Os isotope system to geochemistry and cosmochemistry. *Geochim. Cosmochim. Acta* **61**, 4799–4808.

Walker R. J., Morgan J. W. and Horan M. F. (1995) ^{187}Os enrichment in some mantle plume sources: evidence for core–mantle interaction? *Science* **269**, 819–822.

Wedepohl K. H. and Hartmann G. (1994) The composition of the primitive upper earth's mantle. Kimberlites, related rocks and mantle xenoliths. In *Companhia de Pesquisa de Recursos Minerais*, vol. 1 (eds. H. O. A. Meyer and O. H. Leonardos). Rio de Janeiro, pp. 486–495.

Associate editor: Mark Rehkamper